TWO PHASE MIXING COMPARISON, OIL CONTAMINATION COMPARISON AND MANUFACTURING ACCURACY EFFECT ON CALIBRATION OF SLOTTED ORIFICE METERS

A Thesis

by

SARA A. SPARKS

Submitted to the Office of Graduate Studies of
Texas A&M University
in partial fulfillment of the requirements for the degree of

MASTER OF SCIENCE

August 2004

Major Subject: Mechanical Engineering

TWO PHASE MIXING COMPARISON, OIL CONTAMINATION COMPARISON AND MANUFACTURING ACCURACY EFFECT ON CALIBRATION OF SLOTTED ORIFICE METERS

A Thesis

by

SARA A. SPARKS

Submitted to Texas A&M University
in partial fulfillment of the requirements
for the degree of

MASTER OF SCIENCE

Approved as to style and content by:

Gerald Morrison (Chair of Committee)	Dennis O'Neal (Member)
Stuart Scott (Member)	Dennis O'Neal (Head of Department)

August 2004

Major Subject: Mechanical Engineering

ABSTRACT

Two Phase Mixing, Oil Contamination Comparison and Manufacturing Accuracy Effect on Calibration of Slotted Orifice Meters. (August 2004)

Sara A. Sparks, B.S., Iowa State University

Chair of Advisory Committee: Dr. Gerald L. Morrison

In previous studies the slotted orifice plate has demonstrated superior performance characteristics to those of the standard orifice plate. In this study, these comparisons are investigated further. The response characteristics of the slotted orifice plate to the standard orifice plate and V-Cone for two-phase flows of water and air at various qualities, flow rates, and pressures are shown visually. The effect of oil as it flows through a slotted orifice plate and standard orifice plate are visually documented. The effect of manufacturing accuracy on the slotted orifice plates is investigated as to the effect on the coefficient of discharge, percent change in pressure, and Reynolds number. The slotted orifice plate mixes two-phase flow better than the standard orifice plate and V-Cone. There is a manufacturing effect on the slotted orifice plates; the larger the area of the slots, the larger the discharge coefficient.

DEDICATION

This work is dedicated to Gregory E. and Theresa J. Sparks. Thank you for making arrangements so that I can always focus on schoolwork comfortably. Without your love, support, and encouragement it would have been really difficult to make it through the “weed out” classes, let alone 2 college degrees. Thank you. I love you.

ACKNOWLEDGEMENTS

The author would like to thank her committee chairman, Dr. G. L. Morrison, and committee members, Dr. D. L. O'Neal and Dr. S. Scott, for their time, guidance, and help throughout the project.

The author would also like to thank Sang Hyun Park who never failed to amaze her daily in the Turbo lab. Best of luck in all of your future endeavors.

The author would also like to thank Royal, Rene', and Tillie Benson for being a great support and surrogate family in a town where no one else was known.

TABLE OF CONTENTS

Page

Page

LIST OF FIGURES

Page

Page

Page

Page

LIST OF TABLES

Page

NOMENCLATURE

A	Cross-sectional area at point
A_{PIPE}	Cross-sectional area of pipe
A_{SLOTS}	Total slot area (open)
β	Beta ratio
c	Speed of sound
C_c	Coefficient of contraction
C_d	Coefficient of discharge
C_v	Coefficient of velocity
d	Orifice diameter
D_{pipe}	Inner pipe diameter
Eu	Euler number
γ	Ratio of specific heats
π	Pi constant
g_c	Acceleration due to gravity
k	Calibration factor
K	Flow coefficient
μ	Viscosity
$\dot{m}$	Mass flow rate

M	Mach number
$\dot{m}_{AIR}$	Air mass flow rate
$\dot{m}_{WATER}$	Water mass flow rate
P	Absolute line pressure
ΔP	Pressure drop
H	Height above reference point
R	Universal gas constant
Re	Reynolds number
T	Line temperature
V	Fluid velocity
X	Quality
Y	Expansion factor
β	Beta ratio
ρ	Density
ρ_{AIR}	Air density
ρ_{WATER}	Water density

INTRODUCTION

The standard orifice plate is a common obstruction flow devices that measures the flow rate of a fluid in a pipe. [1] The flow rate is determined by measuring the pressure drop across the plate, and the upstream pressure and temperature. It is very inexpensive and simple to replace. The main disadvantage of the standard orifice plate is its sensitivity to upstream flow conditions. The slotted orifice plate uses the same strategies to measure the flow rate. It is also relatively inexpensive and a drop-in replacement for the standard orifice plate. However, the slotted orifice plate has shown superior characteristics to the standard orifice plate. [2] The slotted orifice plate has proven to have smaller head loss for equivalent beta ratios and flow rates. The pressure recovery downstream of the plate occurs much faster. Smaller eddies are produced upstream and downstream of the plate. There is less dependence upon upstream swirl conditions, and the discharge coefficient tends to stay closer to one.

Flow measurement is a very important process in oil, natural gas and chemical processing industries. Accuracy and repeatability of the flow meters are of high

_____
This thesis follows the style and format of the Journal of Flow Measurement and Instrumentation.

importance in these industries. Knowledge of the flow rates of air, water, and oil in these facilities must be exact in knowing the amount of oil or gas produced. Accuracy of a flow measurement tells whether the quantity measured is the actual true value. Repeatability is a quantitative expression that shows whether a measurement produces the same value of the same quantity when carried out by the same method, by the same observer, with the same measuring instruments, at the same location at appropriately short intervals of time. Accuracy and repeatability will be evaluated for several slotted orifice plates. Flow visualization of air/water and air/oil mixtures passing through the slotted plate will be compared to the standard orifice meter and V-cone, or inverted venturi for the air/water mixture only.

Orifice flow meters are the most widely used flow meters due to the relative low cost, simple construction, and that there are no moving parts. The standard orifice plate is a circular disc that has a hole drilled out at the center. It is mounted in a pipe between two flanges. The inlet side is flat whereas the outlet side is beveled. Fully developed flow that is axially symmetric on the upstream side of the plate is required for the orifice flow meter to be accurate. The standard orifice plate obstructs the flow forcing the fluid to be constricted. As the flow gets closer to the plate, it attains radial momentum and accelerates through the orifice. As the fluid exits the orifice plate, the flow separates creating a recirculation zone on the backside of the plate. The obstruction also creates a

differential pressure. The differential pressure is obtained by measuring the pressure on the inlet and outlet side of the plate. The flow rate of the fluid is proportional to the pressure drop across the plate. This phenomenon is the main motivation behind the study of orifice plate flow meters. The mass flow rate of the fluid is derived using Bernoulli's equation. The flow is assumed to be steady, frictionless, uniform, and incompressible with no body forces. Two locations are considered in this analysis. The first point (1) is located upstream where the orifice plate has no effects on the flow. The second point (2) is located at the vena contracta where the pressure is minimum. Since the edge of the orifice is sharp, the flow tapers so that the actual area through the orifice is not the measured area. This is called a vena contracta. Bernoulli's equation is written as,

$$\frac{P_1}{\rho} + \frac{V_1^2}{2} + gH_1 = \frac{P_2}{\rho} + \frac{V_2^2}{2} + gH_2 \qquad (1)$$

where P_1 (Pa) and P_2 (Pa), V_1 (m/s) and V_2 (m/s), and H_1 (m) and H_2 (m) are the respective pressures, velocities, and heights above the datum at points one and two. The symbol, ρ (kg/m^3), is the constant density of the fluid and g (m/s^2) is the acceleration due to gravity. Assuming both points (1) and (2) are at the same height, then

$$H_1 = H_2 \qquad (2)$$

The continuity equation states that the mass flow rate in and out of the pipe is given by

$$\dot{m} = \rho A_1 V_1 = \rho A_2 V_2 \tag{3}$$

Where $\dot{m}$ (kg/s) is the mass flow rate of fluid flowing through the pipe, and A_1 (m^2) and A_2 (m^2) are the respective cross sectional areas at location (1) and (2). Solving equation (3) for V_1 and substituting it in equation (1),

$$V_2 = \sqrt{\frac{2(P_1 - P_2)}{\rho(1 - (\frac{A_2}{A_1})^2)}} \tag{4}$$

Substituting the expression for V_2 into equation and rearranging the geometric and pressure terms is shown as (3),

$$\dot{m} = \rho A_2 V_2 = \frac{A_2}{\sqrt{1 - \left[\frac{A_2}{A_1}\right]^2}} \sqrt{2\rho\Delta P} \tag{5}$$

The cross section of the vena contracta at point (2) is actually very difficult to measure so it is replaced by the cross sectional area of the orifice. A correction constant called the contraction coefficient, C_c, is multiplied onto the area. Due to the vena contracta and frictional effects, the velocity is altered. Therefore, another correction factor, the coefficient of velocity, C_v, is multiplied to the velocity. The beta ratio is defined as,

$$\beta = \sqrt{\frac{A_{orifice}}{A_1}} = \frac{d_{orifice}}{D_{pipe}} \tag{6}$$

The A_2 in equation (5) is replaced with the area of the orifice. C_c and C_v are also substituted into this equation so that the mass flow rate is given as,

$$\dot{m} = C_c C_v A_{orifice} \left(\frac{1}{\sqrt{1-\beta^4}} \right) \sqrt{2\rho\Delta P} \tag{7}$$

The contraction coefficient and velocity coefficient, C_c and C_v, can combine as the discharge coefficient, C_d. Putting this into the equation and then solving for the coefficient of discharge gives,

$$C_d = \frac{4\dot{m}\sqrt{1-\beta^4}}{\pi (D_{pipe}\beta)^2 \sqrt{2\rho\Delta P}} \tag{8}$$

This coefficient of discharge is calculated from measured values for all of the plates tested. It is plotted against the air Reynolds number and percent change of pressure across the plate. The Reynolds number is given as

$$\mathrm{Re} = \frac{4\dot{m}}{\pi D_{pipe} \mu_{air}} \tag{9}$$

The expansion factor, Y, is a correction for compressible flow effects. [8] The Mach number is the velocity of the fluid divided by the speed of sound through that fluid is also a measure of compressibility. For single-phase flows, the speed of sound is a function of the ratio of specific heats, molecular weight and temperature. For two-phase flows that consist of a liquid and gas, the speed of sound varies from the speed of sound in liquid to the speed of sound in the gas. This variation however is not linear. In fact, the speed of sound can be less than 20% of the individual values of the gas or liquid. Therefore, the expansion factor is not separated from the flow coefficient, K. The expansion factor and flow coefficient are independent of air Reynolds number when calculated using the

air and water densities. This means that KY is only a function of only quality over a range of flow rates. As the quality decreases or water flow rate increases, the KY value increases. So if the quality of a mixture is known, the product of flow coefficient and expansion factor can easily be obtained. By using the density of either the liquid or gas, the total mass flow rate through the slotted orifice plate is determined.

This study investigates how the discharge coefficient for the slotted orifice plate varies with Reynolds number, $\frac{\Delta P}{P}$, and β ratio. Effects of machine reproducibility will also be evaluated.

LITERATURE REVIEW

Dr. Kenneth Hall and Dr. James Holstre of the Chemical Engineering Department at Texas A&M University first developed the idea of a slotted orifice plate to produce a pressure drop in a gas pipeline at the Dansby Power Plant in Bryan, Texas. The pressure drop was needed to allow gas samples to pass through an external analyzer. It was later evaluated as a flow meter. Like the standard orifice plate, the slotted orifice plate is an obstruction or pressure-differential meter that can provide volumetric or mass flow rates. The slotted orifice plate has a circular array of radially aligned slots that extend from the center to the edges of the pipe. The slotted orifice plate has a total area equivalent to that of the single hole of the standard orifice plate for a given beta ratio. The initial purpose of the plate was to provide a differential pressure so that fluid could be sampled and returned to the pipeline without the use of a pump or compressor. The slotted orifice plate was first tested as a flow conditioner by Larry Michael Ihfe [3] and Dr. Gerald L. Morrison at the Mechanical Engineering Department at Texas A&M University. In attempts to develop a new flow conditioner capable of creating a fully turbulent flow profile in a short pipe length, many numerical and experimental studies were performed. It was found that fully developed flow could be obtained in a shorter length of

pipe than in other commercially available flow conditioners. This was done by varying the porosity of the plate across the radius of the pipe. However, the slotted orifice plate was found to be unacceptable as a flow conditioner. Compared to other flow conditioners, the slotted plate created higher permanent head losses.

The focus of studies were then shifted to evaluate the slotted orifice plate as a flow meter rather than a flow conditioner. Terracina [4] and Dr. Gerald L. Morrison investigated the slotted orifice plate when subjected to single-phase flow, using both numerical and experimental data. The study investigated the effects of velocity profile distortions, line pressure, mass flow rate, tube bundle location, and pipe size scaling. It was determined that the slotted orifice plate possessed better accuracy than the standard orifice plate when subjected to ill-conditioned flows. By decreasing the slot width to plate thickness ratio to 0.25, the results showed even better immunity to the variation in upstream flow conditions and eliminated the need for tube bundles. It was decided to use the square inlet for future research when compared to round contours that produced high differential pressures and the beveled inlet.

The slotted orifice plate has demonstrated superior performance over the standard orifice plate when used as a single-phase flow-metering device. The slotted orifice meter has shown reduced dependence upon upstream flow

conditions. [5] The slots in the slotted orifice plate reduce head loss across the plate due to the increased perimeter to area ratio. This causes faster pressure recovery and a shorter recirculation zone [6]. The pressure recovers within one pipe diameter. However, the pressure recovery for the standard orifice plate recovers at 3.5 pipe diameters downstream of the plate for a 0.5 beta ratio.

Research has also shown that the slotted orifice does not depend upon the inlet velocity profile and very little upon swirl. Morrison et al. [7] evaluated the performance of air through a standard orifice plate and slotted orifice plate each with a beta ratio of 0.50. The two flow meters were tested at air Reynolds numbers of 54,700 and 91,100 in 0.0504 m (2 in.) diameter pipe. The airflow was preconditioned using a concentric tube flow conditioner in order to produce varying axial velocity profiles without swirl. When the velocity profile was biased towards the pipe wall, the pressure differential across the standard orifice plate increased. When the flow was concentrated along the pipe centerline, the pressure actually decreased since less force is required to flow through the hole. However, the slotted orifice plate was shown to be insensitive to the inlet velocity profile. The discharge coefficient for the slotted orifice plate was close to unity and varied within 0.25% accuracy while the standard orifice plate at the same condition varied up to 6% for maldistributed flows [8]. A swirl generator upstream of each orifice plate produced adverse flows with variable amounts of swirl. The slotted and the standard orifice plate flow meters were tested. The

slotted orifice meter once again showed superior results to that of the standard orifice plate. The discharge coefficient for the standard orifice plate was found to increase up to 5% with the increase in amount of swirl. However, the discharge coefficient for the slotted orifice plate decreased by a maximum of 2% with an increase in the amount of swirl. Consequently, when a swirl generator created swirl angles of 20 degress or less, the discharge coefficient of the slotted orifice plate varied less than 0.5% of that for the well-conditioned flow case. Therefore, the slotted orifice plate resulted in discharge coefficients that were once again closer to unity.

Macek [9], under the advisement of Dr. Gerald L. Morrison, ran many tests comparing the slotted orifice plate and standard orifice plate as a single phase flow meter. Macek [9] investigated thickness effects of the slotted orifice plate in a 5.08 cm (2 inch) diameter pipe. He found that a slotted orifice plate with a thickness of 6 mm (0.235 in.) ensured that the pipe wall pressure distributions were more consistent than 3 mm (0.118 in) regardless of upstream flow conditions. The plates with 6 mm (0.236 in.) thickness also produced a lower overall pressure drop than plates with a 3 mm (0.118 in.) thickness.

Brewer [10], under the direction of Dr. Morrison, constructed a two-phase flow facility using water and air to evaluate the slotted orifice plates with beta ratios of 0.50 and 0.43. Pure air (100% quality) to slug flows (20% air quality) were

evaluated. Video documentation was made of the flow for different qualities and pressures for horizontal and vertical orientation. Brewer also investigated the dependence of location of pressure taps in order to measure the differential pressure across the plate. Flange taps or 2.5 pipe diameter taps located upstream and downstream of the slotted orifice plate were both found to be accurate. Compressibility effects were found to have different responses for the two beta ratios tested. At either horizontal or vertical orientations of the plates, the discharge coefficient was found to be independent of air Reynolds number when plotted as a function of quality based on mass. The discharge coefficient can be expressed as a function of the Euler number and Beta ratio rather than the Reynolds number, Beta ratio, and pipe diameter [11]. This eliminates the pipe diameter and fluid viscosity from the discharge coefficient to form a simplified equation [11]. It was determined that a slotted orifice meter can be used as either a densitometer or a volumetric flow meter for one or two-phase flows [11].

Flores [6] along with Dr. Gerald L. Morrison studied the repeatability and reproducibility of the slotted orifice plate for wet steam flows. The slotted orifice plate proved to be reproducible by testing three beta ratios of 0.43, 0.467, and 0.5 with different working fluids, instrumentation, and line pressures. These factors were found to be independent of the mixture Reynolds number when the calibration factor was plotted as a function of Euler number. The Euler number

is a function of mixture density, mixture mass flow rate, and differential pressure across the slotted orifice plate. The equation is shown as,

$$Eu = \frac{g_c * \Delta P}{\rho * V^2} \quad (10)$$

The calibration coefficient, KY, was determined as,

$$KY = \frac{4\dot{m}}{\pi (D_{pipe}\beta)^2 \sqrt{2\rho\Delta P}} \quad (11)$$

where, K is the flow coefficient, Y is the expansion factor. The quality, steam Reynolds number, and beta ratio were all varied, yet three trends remained the same as those exhibited by the air and water studies performed by Brewer. These trends include that as the gas Reynolds number increases, the differential pressure across the slotted orifice plate increases. The differential pressure increased as the quality decreased. The third trend is that as the gas Reynolds number and quality remained constant, the smaller beta ratio displayed higher differential pressures.

Muralidharan [12] under the supervision of Dr. Gerald L. Morrison studied the response of the slotted orifice plate as a two-phase flow meter with air and water as the working fluids. The quality was varied to determine the effects on the differential pressure and the coefficient of discharge on the slotted plates. The effects of the gas Reynolds number on the coefficient of discharge were also

looked at, as well as the behavior of the coefficient of discharge at low differential pressures. The 0.430 and 0.467 beta ratio slotted plates were tested with different arrangements to evaluate repeatability and reproducibility. The standard orifice plate and venture were compared to prove that the slotted orifice plate exemplifies superior qualities.

OBJECTIVES

Three studies were conducted. The purpose of the first study is to evaluate the effect of manufacturing accuracy and repeatability on the slotted orifice meter calibration for plates with beta ratios of 0.467 and 0.430. The other two studies are flow visualization studies. They directly compare the slotted and standard orifice meters. Water and air mixtures are recorded to compare a slotted orifice plate, standard orifice plate and a V-Cone at different line pressures and mass flow rates. This shows how well each apparatus mixes the water and air before and after entering the slotted orifice plate. The test conditions will contain the same air Reynolds number and qualities used by Brewer. The video resolution is much better than those made by Brewer. The oil and air visualization study shows on camera the effects of oil build up on the slotted and standard orifice plate over time. The steps in determining the objectives are:

1. Determine if there is a geometric discrepancy between plates or if manufacturing standards are adequate by optically measuring the area of each slot and total open area of each slotted orifice plate.

2. For the plates examined in step 1 determine the repeatability of the discharge coefficient when subjected to a variety of air flow rates and line pressures.
3. Determine if there is a correlation between any discrepancies in the flow meter calibration data and the area measurements.
4. Determine how the differential pressure across the plate changes due to oil build up for the slotted and standard orifice plates.
5. Visualize how water and air mixes while flowing through a standard orifice plate, slotted orifice plate and V-cone at different pressures and flow rates.

EXPERIMENTAL APPARATUS

This section contains descriptions of the key components of the test facility located within the Turbomachinery Laboratory. Three different test configurations were used. One was for the manufacturing repeatability test, another for the oil and air flow visualization study, and the last for the water and air flow visualization study. The air flow route will first be described for the facility. The stainless steel pipe repeatability test section will then be explained along with the acrylic pipe water and air flow visualization test section, oil and air flow visualization test section, and instrumentation used for the flow visualization tests.

Orifice Plates

The 0.430 and 0.467 beta ratio slotted orifice plates will be investigated in these studies. The 0.467 beta plate has 26 holes while the 0.430 beta plate has 32 smaller holes that make up less area for fluid to flow through. They are shown respectively in Figure 1 and Figure 2. Each plate has four flange bolt holes that are equally spaced apart. This allows a bolt, washer, and nut to hold the plate tightly in place between the pipe flanges. The two flange locator pins are used

to line the orifice plates correctly to the flange. The three orifice plate locator pins are used to line up the 3 mm (0.118 inch) acrylic orifice plates that are used for the visibility tests to ensure that the plates are exactly lined up. Two of the 3 mm (0.118 inch) plates are needed to get the thickness of 6 mm (0.236 inch) as Macek had investigated. The plates used for the repeatability test are made out of stainless steel and have a thickness of 6.35 mm (0.25 inches) so that only one plate is needed with no orifice plate locator pins. The standard orifice plates used in this study are shown in Figure 3. The V-Cone, an inverted venturi, is also compared against in the water and air visibility study.

Air Flow Facility

Two oil-free Ingersoll-Rand air compressors supply air at about 724 kPa (105 psi) from a compressor facility outside the laboratory. A pair of desiccant dryers filter and dry the compressed air to a dew point temperature of –40 degrees Celsius (-40 degrees Fahrenheit). The air is brought into the laboratory facility through a 10.16 cm (4 inch pipe). Once the air enters the laboratory facility, it is directed through a 5.08 cm (2 inch) rubber hose. For the repeatability test and water and air flow visualization test, the air is directed to a 5.08 cm (2 inch) stainless steel pipe. The air pressure, temperature, and volumetric flow rate are measured using two independent turbine flow meters. The line pressure is measured with a Rosemount Model 3051C SMART absolute pressure transducer measures the line pressure. It has a pressure span of 10.3421 to

1034.21 kPa (41.5198 to 4151.98 in H_2O). The Rosemount absolute pressure transducer has an accuracy of 0.075% of the span. [8] Once the initial measurements have been made, the air flows through an electromechanical control valve (Masonelian Model 35-35212 electro-pneumatic valve). This valve regulates the air flow. From the Masoneilan valve, the air continues to flow through 5.08 cm (2 inch) stainless steel pipe to 5.08 cm (2 inch) rubber hose and then through 5.08 cm (2 inch) PVC pipe where the orifice plate is located in either an acrylic test section for the water and air flow visualization study or in stainless steel piping for the repeatability studies. Figure 4 shows this set-up. The air flows through the orifice test section then exits through a 5.08 cm (2 inch) rubber hose to another Masoneilan valve that controls the back pressure. The air is then released outside to the atmosphere.

For the oil and air flow visualization study, the air mass flow rate was controlled through a sonic nozzle bank consisting of three sonic nozzles (Model N24018-SI (150) N240127-SI (150) and N240255-SI) mounted in parallel. The Colorado Engineering Experiment Station Incorporated (CEESI) initially calibrated the nozzles. CEESI makes use of standards traceable to the National Institute of Standard and Technology (NIST). The air enters the lab facility through the 10.16 cm (4 inch) pipe. It is connected to the three sonic nozzles by a 5.08 cm (2 inch) rubber hose. An Omega Model PX236 pressure transducer is placed upstream of the sonic nozzle bank to monitor the pressure. A T-type

thermocouple measures the temperature of the air. The set of converging nozzles accelerates the air to a choked state. This means that the air is flowing at the speed of sound or a Mach number equal to one at the exit. Given the choked state along with the pressure and temperature of the air, the mass flow rate is determined by using the gas dynamics equation:

$$\dot{m} = \frac{PA}{RT} M \sqrt{\gamma RT} \qquad (12)$$

This mass flow rate is a repeatable constant that can be changed operating the three sonic nozzles individually or in combination with one another. The three sonic nozzles have individual air mass flow rates of 0.0141 kg/s (0.0311 lb/s), 0.02785 kg/s (0.0614 lb/s), and 0.0558 kg/s (0.123 lb/s). The first and second sonic nozzles produce an air mass flow rate of 0.2037 kg/s (0.0924 lb/s). The second and third sonic nozzles produce an air mass flow rate of 0.0835 kg/s (0.184 lb/s). One and three give 0.0699 kg/s (0.154 lb/s), and all three sonic nozzles operated together produce the maximum air mass flow rate of 0.0975 kg/s (0.215 lb/s). Once the air has passed through the sonic nozzle bank, 5.08 cm (2 inch) PVC pipe carries the air to clear acrylic pipe where the orifice plate section is located. An oil separator follows the orifice plate before the air is brought to the atmosphere. The set up is shown in Figure 5.

Manufacturing Repeatability Test Section

The airflow follows the first path described above. A T-type thermocouple is located 53.34 cm (21 inches) upstream of the slotted orifice plate. Just past the thermocouple is a strainer that catches any fluid or solid particles flowing through the line. In order to measure the differential pressure through the slotted orifice plate, flange pressure taps are used. The flanges are bolted together with gaskets that surround the orifice plate on each side. The lettering on the slotted orifice plate faces upstream. Two different slotted orifice plate beta ratios were investigated: the 0.430 and 0.467 beta ratios. Two Honeywell digital multi-variable transducers are connected in parallel to the pressure taps. They measure the temperature, upstream pressure, and differential pressure across the slotted plate. The first Honeywell is calibrated for a differential pressure of 69 kPa (10 psi) and the second for a 6.9 kPa (1 psi) pressure drop across the plates. The airflows out of the meter run through a 5.08 cm (2 inch) rubber tube to a Masoneilan valve that controls the backpressure.

Water and Air Flow Visualization

For the water and air visibility study, the air flows through the same path as the repeatability study. Therefore the mass flow rate is controlled with the two

Masoneilan valves. However, the orifice plate is located in an acrylic 5.08 cm (2-inch) pipe instead of the stainless steel pipe. The acrylic test section is constructed of 50.8 mm (2 in.) ID acrylic pipe with a wall thickness of 6.36 mm (0.25 in.) Two 12.7 mm (0.5 in.) thick acrylic slotted orifice plates were located between the flanges. The two plates are aligned with two locator pins or dowels and sealed together with silicon vacuum grease in order to keep the plates in place throughout the test. The silicon vacuum grease also helped prevent leakage of water or air between the plates.

The water is added in the PVC portion of the pipe that is connected just upstream of the acrylic test section. Figure 6 shows a diagram of the water flow. The water is supplied from a 0.756 m^3 (26.7 ft^3) tank. A pump draws the water from the tank into two parallel pipes. Each pipe has a different size Coriolis flow meter attached to it. One Coriolis flow meter measures large flow rates while the other measures smaller flow rates. The small Coriolis flow meter has a range of 1.512×10^{-3} to 0.03 kg/sec. The large Coriolis flow meter has a range of 0.03 to 0.65 kg/sec. Each Coriolis flow meter is attached to a transmitter that converts the flow rate into a current signal ranging from 4 to 20 mA. This transmitter measures the mass flow rate, volumetric flow rate, and density of the flow. Downstream of the small Coriolis meter (Model CMF010) are two needle valves to adjust the liquid flow rate. An automatic control valve (Masoneilan Model 2800 Series) is used to control the flow through the large Coriolis meter.

The needle valves are connected to DC motors by a rigid coupling. The needle valve is controlled by a knob and toggle switch in the control room. The water exits the flow meters through a rubber hose that is connected to the PVC pipe where it mixes with the air flowing through the test section. The water and air mixture flows through a standard orifice plate, slotted orifice plate or a V-Cone. A video camera is set up to record the inlet of the flow meter. It is then repositioned to record the outlet mixing conditions. The air and water mixture exits through another 5.08 cm (2-inch) rubber tube to the second Masoneilan valve that controls the backpressure. The water and air are returned to the same tank so that the water can be recirculated. The air is exhausted to atmosphere.

Oil and Air Mixture Visualization

The air for the oil and air visualization study supplied by the air compressor flows through a set of 3 sonic nozzles. The air pressure and temperature are measured upstream of the sonic nozzle bank. The air then flows through the sonic nozzles that are followed by ball valves. Opening valves and varying the air supply pressure adjust the flow rate. The air flows through a 5.08 cm (2-inch) acrylic pipe test section where a fine mist of vegetable oil is sprayed into the center of the pipe to mix with the airflow. A pressurized paint can that holds a constant pressure throughout the duration of the test supplies the oil flow. The

air and oil mixture flows through a clear slotted or standard orifice plate. A differential pressure transducer is used to measure the pressure differential across each plate. A multi-meter was placed in the field of view to allow recording of the pressure differential. A video camera was positioned to record the oil flow through the plate. A mirror on the backside of the slotted plate is also shown in the camera view along with the voltage reading. An oil separator gathers the oil before the air is released outside to the atmosphere.

EXPERIMENTAL PROCEDURE

Calibration of the Pressure Transducers

All of the pressure transducers are calibrated with an Ametek Model RK-300 pneumatic deadweight tester. The pneumatic dead weight tester is attached to the high-pressure ports of the pressure transducers. The low-pressure ports of the pressure transducers are open to atmosphere during calibration. The Rosemount pressure transducers are calibrated for 0 to 690 kPa (0 to 100 psi). The Honeywell digital multi-variable transducers are also calibrated to determine accuracy of the digital reading. One transducer ranges from 0 to 69 kPa (10 psi) while the other measures from 0 to 6.9 kPa (1 psi). The digital output values correspond to the deadweight tester pressure. The calibration is performed by applying weights to the deadweight tester. This weight is equivalent to a specific amount of pressure. The corresponding voltages produced by the analog pressure transducers are attained. The pressure is then plotted versus the voltage. A linear curve fit is applied to the plot. The subsequent equation of the line is the calibration of the pressure transducer.

Data Acquisition System

The thermocouple, volumetric flow rate, and Rosemount pressure transducers produce a voltage output that are connected to a data acquisition board which converts the analog signal to a digital reading. The Lab VIEW graphical program developed and marketed by National Instruments, Inc. is used to design a virtual instrument program used in the data acquisition. The Lab VIEW program records the digital reading. The Honeywell multi-variable transducers produce direct digital output that is recorded by a RGC circuit board that is interfaced to a separate laptop computer. The laptop records data every second to an output file that is overwritten each time. This output file is shared with the data acquisition board through Network Neighborhood. It is read into the same Lab VIEW program.

Every 500 milliseconds the Lab VIEW program records the air supply pressure, Daniel turbine meter, thermocouple, and Honeywell multi-variable data. Opening and closing the Masoneilan valves control the upstream pressure and volumetric flow rate.

Slotted Area Calculation

A Hewlett Packard ScanJet ADF Scanner optically scanned each slotted plate. The resolution was set to 2400 x 2400 pixels per square inch. The highlights, shadows, midtones, grayscale, and intensity were all kept constant for all of the scans to create comparable results between the various plates. Sigma ScanPro 5, image measurement software that calculates the area of each slot and the total area of the slots, analyzed the scans. Area distributions of each plate were plotted and compared. The data of each plate is then compared to the discharge coefficient repeatability data.

Repeatability Test Procedure

The two compressors are turned on and the valve to the test section is opened. The shop air valve is also turned on so that the Masoneilan valves may be actuated. Turning a knob in the control room opens the Masoneilan valves. The upstream and downstream Masoneilan valves are controlled to result in a specific pressure and flow rate. The pressure is kept at a constant 275 kPa (40 psi), 414 kPa (60 psi), and maximum pressure while the volumetric flow rate for each pressure is varied from 0.00472 m^3/s to 0.0425 m^3/s (10-90 cubic feet per

minute) in increments of 0.0047 m^3/s (10 cfm) measured at the compressor supply pressure. When the pressure and volumetric flow rate are at steady state for about 4 minutes, a data point is taken every 500 milliseconds. Seven hundred data points are then averaged and saved in a data file. The atmospheric pressure is recorded for each test to allow accurate absolute pressure calculation. The density and data file are utilized by MathCAD to calculate the following characteristics of the flow:

- Reynolds number
- Euler number
- Discharge coefficient
- Upstream pressure
- Differential pressure in kilopascals and inches of water across the slotted orifice plate
- Percent of change of pressure across the slotted orifice plate $\left(\frac{\Delta P}{P}\right)$
- Density
- Velocity
- Volumetric flow rate

This MathCAD data is recorded to a file that is imported into 3-D Table curve software program. The discharge coefficient is curve fit as a function of

Reynolds number and percent change of pressure drop. This procedure was repeated for 8 plates with a beta ratio of 0.430 and 5 plates with a beta ratio of 0.467.

Water and Air Flow Visualization Procedure

The standard orifice plate is placed between the flanges. The air pressure is set to a constant absolute pressure of 310 kPa. The air volumetric flow rate is set at an approximate air Reynolds number of 60,000 while the water mass flow rate is varied at:

- 0.0042 kg/s (0.55 lb/min) (90% air quality)
- 0.014 kg/s (1.8 lb/min) (70% air quality)
- 0.072 kg/s (9.5 lb/min) (30% air quality)

The air volumetric flow rate is set to an approximate Reynolds number of 158,000 with the water flow rate set at:

- 0.0104 kg/s (1.38 lb/min) (90% quality)
- 0.124 kg/s (16.4 lb/min) (40% quality).

The final air volumetric flow rate for the standard orifice plate is set at an approximate Reynolds number of 205,000. The water flow rates are:

- 0.013 kg/s (1.7 lb/min) (90% quality)

- 0.047 kg/s (6.16 lb/min) (70% quality).

Steady state flow conditions were obtained at each of these values. Approximately 10 seconds of video is recorded upstream and downstream of the plate at each flow condition. This visually shows how the air and water mixture enters and exits the plate.

A V-cone (inverted venturi) is documented the same way. Once again the air pressure is set to 310 kPa. The air mass flow rate is maintained at an approximate air Reynolds number of 60,000. The water flow rates are set at:

- 0.003 kg/s (0.4 lb/min) (90% quality)
- 0.013 kg/s (1.7 lb/min) (70% quality)
- 0.033 kg/s (4.38 lb/min) (50% quality)

The air volumetric flow rate is set to an approximate Reynolds number of 158,000. The water mass flow rate is set at:

- 0.00945 kg/s (1.25 lb/min) (90% quality)
- 0.0370 kg/s (4.9 lb/min) (70% quality)
- 0.128 kg/s (16.9 lb/min) (40% quality)

The air volumetric flow rate is set to an approximate Reynolds number of 205,000. The water mass flow rate is set at:

- 0.0136 kg/s (1.8 lb/min) (90% quality)
- 0.0466 kg/s (6.16 lb/min) (70% quality)

The slotted orifice meter is placed between the flanges and documented as the other two meters. The air pressure is set at a constant 310 kPa. The airflow rate is set to an approximate air Reynolds number of 60,000. The water flow rates are set from 90% to 20% quality as shown below:

- 0.0045 kg/s (0.6 lb/min) (90% quality)
- 0.0083 kg/s (1.1 lb/min) (80% quality)
- 0.014 kg/s (1.9 lb/min) (70% quality)
- 0.0210 kg/s (2.8 lb/min) (60% quality)
- 0.0320 kg/s (4.2 lb/min) (50% quality)
- 0.0490 kg/s (6.5 lb/min) (40% quality)
- 0.076 kg/s (10.1 lb/min) (30% quality)
- 0.140 kg/s (17.9 lb/min) (20% quality)

An approximate air Reynolds number of 158,000 is set. The water mass flow rate varies from 90% to 25% as shown below:

- 0.010 kg/s(1.35 lb/min) (90% quality)
- 0.0220 kg/s (2.9 lb/min) (80% quality)
- 0.036 kg/s (4.7 lb/min) (70% quality)
- 0.058 kg/s (7.7 lb/min) (60% quality)

- 0.084 kg/s (11.1 lb/min) (50% quality)
- 0.124 kg/s (16.4 lb/min) (40% quality)
- 0.197 kg/s (26.1 lb/min) (30% quality)
- 0.264 kg/s (34.9 lb/min) (25% quality)

An approximate air Reynolds number of 205,000 was obtained. The water mass flow rate varies from 90% to 55% air qualities as shown below:

- 0.011 kg/s (1.5 lb/min) (90% quality)
- 0.030 kg/s (3.95 lb/min) (80% quality)
- 0.048 kg/s (6.3 lb/min) (70% quality)
- 0.076 kg/s (10 lb/min) (60% quality)
- 0.089 kg/s (11.8 lb/min) (55%quality)

Once all of the data is recorded, the videos are transferred digitally to a computer. A DVD videodisk is produced to show how the flow fields vary.

Oil and Air Procedure

The oil weight in the reservoir at the beginning of the test is measured. Sonic nozzles 1 and 2 are opened producing an air Reynolds number of 54,700 and mass flow rate of $6.99*10^{-4}$ kg/s (0.0924 lb_m/s). The air pressure is set at a constant 103 kPa (15 psi) while the oil pressure is set at a constant 207 kPa (30

psi). The video camera records the slotted orifice meter and voltmeter for 90 minutes. The oil weight is then measured again to obtain the average oil mass flow rate. After the video is filmed, the voltage reading is plotted every 2 minutes to show the change in pressure drop across the slotted orifice plate with respect to time. This exact same procedure was repeated with the standard orifice meter for 60 minutes.

RESULTS AND DISCUSSION

Water and Air Flow Visualization Results

The slotted orifice meter, standard orifice meter, and V-Cone video data were made into a DVD. The DVD shows the three different meters that may be selected to view on the main menu. Each series runs through about 10 minutes of video documentation that shows all of the flow conditions mentioned above. A slide flashes on the screen before each flow condition is run. It shows the upstream air pressure, air mass flow rate, water mass flow rate and the quality of the two-phase mixture. The water and air mixture is shown upstream of the plate and then downstream of the plate to show the effect of the plate. For lower flow rates, the water of the two-phase flow generally tends to flow on the bottom of the pipe upstream of the plate. This is called stratified flow. An example of stratified flow is shown in Figure 7. This figure shows a constant upstream air pressure of 310 kPa (45 psi), an air flow rate of 0.009 m^3/s (19 cfm), a water mass flow rate of 0.003 kg/s (0.4 lb/min) with an air quality of 90%. The water is clearly seen to flow on the bottom of the pipe. Once the water and air mixture passes through the slotted orifice meter, the 2-phase mixture becomes much more evenly dispersed throughout the cross section of the pipe and therefore

mixed. This is shown in Figure 8. As the water mass flow rate increases to 0.050 kg/s (6.5 lb/min) with a quality of 40%, the majority of the water is still stratified though water is starting to disperse throughout the air stream. Drops are shown flowing along the walls of the pipe. This is shown in Figure 9. The water and air mixture is again shown to be very well mixed downstream of the slotted orifice plate as seen in Figure 10. More water begins to mix in with the air flow as the water mass flow rate increases. At 20% quality, more water is seen flowing along the walls. This is shown in Figure 11. When the air pressure is increased to (50 cfm), droplets of water already appear on all sides of the wall with 90% air quality as shown in Figure 12. Figure 13 shows that the water is mainly stratified upstream of the slotted orifice meter. Once the water exits the slotted orifice plate, the water is completely mixed. As the upstream air pressure and water mass flow rates increase, the two-phase flow becomes annular. This is shown in the upstream view of Figure 14. The downstream view, Figure 15**,** shows that the water/air mixture is very well mixed. The downstream view of 0.02 m^3/s (50 cfm) with a quality of 50%, Figure 16, shows that the water/air mixture is very well mixed in the axial and radial direction as is the 30% quality flow mixture. An upstream air flowrate of 0.030 m^3/s (65 cfm) was set. At 80% quality the upstream flow is annular. The water flows in a very straight motion along all sides of the pipe as seen in Figure 17. Once the water passes through the slotted orifice plate, the water and air consistently mixes throughout the pipe as shown in Figure 18. There are no water gaps present on the side of the pipe

as shown upstream. At 0.030 m^3/s (65 cfm), qualities 70% to 55% exemplify very similar characteristics. The upstream flow is annular and the downstream flow is completely mixed.

The standard orifice plate was also run at an air flow rate of 0.009 m^3/s (19 cfm) and 90% quality. Since the water is stratified at these conditions, the water flows up the plate and then splashes out in fast pulses to mix with part of the air flow. The downstream conditions are shown in Figure 19. Notice that water gathers on the bottom of the pipe in the large recirculation zone. The standard orifice plate does not mix as well as the slotted orifice plate at the low water mass flow rates. Figure 20 (0.009 m^3/s, 70% quality) shows how the upstream flow is stratified at this condition. The water flows straight up the plate and then exits at the top of the orifice. The downstream view is shown in Figure 21. The two-phase mixture at this point is mixed much better than the lesser qualities at this air flow rate since more water is being added. When the flow rate is raised to 0.020 m^3/s (50 cfm), the upstream flow at 90% quality is once again stratified. The downstream flow mixes well though there does not tend to be as much turbulence and uniform mixing throughout the pipe occurring as does with the slotted orifice plate. Views of both the upstream and downstream flow conditions are pictured in Figure 22 (0.020 m^3/s, 90% Quality). There is annular flow with turbulent, uniform mixing taking place downstream of the standard orifice plate at 40% quality. At higher flow rates and lower air qualities, the

slotted orifice plate tends to display qualities more similar to the slotted orifice plate. This is pictured in Figure 23 (0.020 m^3/s, 40% Quality). At a air flow rate of 0.030 m^3/s (65 cfm) and quality of 90%, the upstream and downstream flows are annular as is the case for 70% quality. These pictures are in Figure 24 and Figure 25.

The V-Cone was tested at the same upstream conditions as before with an air flow rate of 0.009 m^3/s (19 cfm) and 90% air quality. Figure 26 shows that the majority of the water entering flows on the bottom of the pipe with large droplets flowing throughout the rest of the pipe. The flow downstream of the V-Cone is stratified. It mixes less than the slotted and standard orifice plates at the low flow rates. As the water mass flow rate is increased, the water seems to pulse out of the V-Cone in spurts. The air and water mixture does mix better than it does at the lower flow rates. It is no longer stratified though the water shoots out heavy in only a couple sections, not evenly throughout the cross section of the pipe. 50% quality is shown in Figure 27. As the water mass flow rate is increased to an air quality of 30%, the water shoots out of the V-Cone so that mixing appears to occur in the flow direction, not necessarily along the radius of the pipe and appears to be swirling. A clip of this is shown in Figure 28 (0.009 m^3/s, 30% Quality). At a flow rate of 0.020 m^3/s (50 cfm) and 90% air quality, the flow upstream is annular though not evenly mixed throughout the pipe. The flow exits the V-Cone very similarly to how it entered the V-Cone. This is shown

in Figure 29 (0.020 m^3/s, 90% Quality). Figure 30 (0.020 m^3/s, 70% Quality downstream view) shows that the two-phase mixture is much more evenly mixed than at the lower flow rates though water flows heavier along the bottom than the sides and top. At a flow rate of 0.030 m^3/s (65 cfm) and 90% air quality, Figure 31, shows that the two-phase flow mixture behaves similarly upstream and downstream of the V-Cone. There are heavy streaks of water located throughout the pipe that flow in a very straight path that shows no turbulent mixing once it has exited the V-Cone.

Oil and Air Flow Visualization Results

The oil and air flow visualization test set-up that was seen through the video camera is shown in Figure 32 for the slotted orifice plate. The weight of the oil reservoir was measured before and after the test. A mass of 0.44452 kg (0.98 pounds) of oil flowed through the slotted orifice meter in 5425 s (90.4 minutes). 0.349 kg (0.77 pounds) of oil flowed through the standard orifice meter in 3704.4 s (61.74 minutes). This determined the oil mass flow rate through the plates. The oil mass flow through the slotted orifice plate is $8.1954*10^{-5}$ kg/s (0.01084 lb/min) and $9.4285*10^{-5}$ kg/s (0.01247 lb/min) through the standard orifice plate.

The oil flowed with a constant air flow rate through the acrylic pipe. The upstream and downstream views of the oil and air flowing through the orifice

plates were recorded on video along with the differential voltage reading. The video was paused every two minutes to record the voltage reading. The voltage corresponds to the differential pressure drop across the plate. The differential pressure drop graphs are plotted versus time on Figures 33 and 34 for the standard and slotted orifice plates. The standard orifice plate differential pressure has a steep upward slope in the first ten minutes and then stays at a constant value for throughout the rest of the test.

The slotted orifice plate has a higher differential pressure results than the standard orifice plate. This absolute difference in differential pressure is expected due to the fact that the slotted orifice plate has a beta ratio of 0.430 as opposed to the standard orifice plate that has a beta ratio of 0.500. The differential pressure for the slotted orifice plate decreases rapidly for the first ten minutes. This effect is opposite of the standard orifice plate. The next 65 minutes of the test then varies between approximately 23.20 and 23.40 kPa, this is more variance than the standard orifice plated showed. At 75 minutes the differential pressure drops off to about 23.15 kPa for the remainder of the test.

The discharge coefficients for the standard and slotted orifice plates are plotted respectively versus time in Figures 35 and 36. The standard orifice plate has an initial discharge coefficient of about 0.675. It then decreases for the first ten minutes and then remains around a constant value of 0.672. The slotted orifice

plate discharge coefficient is initially at 0.675. It increases for the first ten minutes and then varies between approximately 0.697 and 0.705 for the remainder of the test.

The oil and air mixture behaves differently than the water and air mixture. At the flow conditions run for the oil and air test, the water and air mixture would be stratified. However, the oil and air behaved in an annular manner. The total, inside surface area of the pipe was covered with oil.

Repeatability Test Results

The single phase air flow experimental data is imported from MathCAD to a 3-D Table curve software program. The discharge coefficient is plotted versus the Reynolds number and percent change of pressure drop across the slotted orifice plate. This 3-D curve is fitted with four coefficients with the equation,

$$C_d = a\left[1 - b\left(\frac{dP}{P}\right)^c\right]\left[1 - \frac{d}{\ln(\mathrm{Re})}\right] \qquad [13]$$

The four coefficients are presented for the 0.430 beta ratio and 0.467 beta ratio in Table 1 and Table 2. The slotted plates with a beta ratio of 0.430 and 0.467 are analyzed and compared in separate tables. It was found in previous research that equation [13] could be simplified by replacing the (c) coefficient

with a constant 1.0365. This reduces the coefficients in the equation down to only three as shown,

$$C_d = a\left[1 - b\left(\frac{\Delta P}{P}\right)^{1.0365}\right]\left(1 - \frac{d}{\ln(\mathrm{Re})}\right) \qquad [14]$$

The discharge coefficient is plotted again versus the Reynolds number and percent change in pressure drop across the slotted orifice meter using 3-D Table curve software that curvefits the data to Equation 14. This solves the three coefficients (a), (b), and (d) and linear regression value. The coefficients are tabulated for the beta ratio 0.430 data in Table 3 and 0.467 data in Table 4. The (a) coefficient for the 0.467 data varies from 1 to 0.93. The percent change of pressure coefficient (b) varies between 0.75 and 0.92 with the median around 0.84. However the Reynolds number coefficient (c) varies from 1.25 to as low as 0.189 with no known reason. This scatter was deemed unacceptable.

Therefore, the next step was to leave out the Reynolds number dependence. So a 2-D graph of the discharge coefficient and percent change in pressure across the slotted plate was made. The equation that was curve fit to this data is shown in Equation 15.

$$C_d = a\left[1 - b\left(\frac{\Delta P}{P}\right)^{1.0365}\right] \qquad [15]$$

The (a) and (b) coefficients were tabulated for each plate. The percent change of pressure coefficient (b) in Equation [15] is a fairly constant value for both the

0.467 and 0.430 beta ratio slotted plates. The 0.467 beta ratio slotted plate (b) coefficient was averaged to 0.817676. The 0.430 beta ratio slotted plate (b) coefficient averaged to 0.781069. The data for the 0.430 and 0.467 beta ratio coefficients (a), (b) and R^2 value are shown in Table 5 and Table 6.

The Reynolds term coefficient was then put back into the equation as shown in Equation 16 along with the averaged (b) coefficient for the 0.430 and 0.467 beta plates stated above. The (a) and (d) coefficients were determined by plotting the coefficient of discharge versus the percent change in pressure and the Reynolds number and then curve fitting the following equation through it,

$$C_d = a\left[1 - 0.817676\left(\frac{\Delta P.}{P}\right)^{1.0365}\right]\left[1 - \frac{d}{\ln(\mathrm{Re})}\right] \qquad [16]$$

The analysis shows that the Reynolds term, d, ranges from a negative 0.18195 to a positive 0.981475 for the 0.467 beta ratio slotted orifice plate. The 0.430 beta ratio slotted orifice plate Reynolds term, b, ranges from –0.78613 to 1.091425. The 0.467 and 0.430 beta ratio coefficients are shown respectively in Table 7 and Table 8. These results were once again unacceptable. Coefficient (a) varied too much for each plate.

Therefore the discharge coefficient was plotted versus the percent change in pressure in a 2-D graph once again across the slotted orifice plate. These data show that as the Reynolds number increases, C_d increases nonlinearly,

asymptoting to a value that is relatively independent of Reynolds number. This is the same behavior seen for a standard orifice plate. In Figures 37 and 38 this behavior can be observed. Therefore, the upper limit of C_d for each plate was observed and a straight line was hand fit. The intercept of this line with the zero $\Delta P/P$ line was recorded. The y-intercept, also know as coefficient (a), of each line is recorded. The discharge coefficient was divided by this y-intercept, (a) value. This ratio is plotted against the percent change in pressure difference. The 0.430 beta plate data forms a data set where the data of all of the plates exactly overlap. This is shown in Figure 39. These data prove to be very reproducible. The data crosses the y-axis at approximately one. The data then lowers to about 0.9 of the discharge coefficient ratio by about 12% change in pressure across the plate. There is some scatter near the lower differential pressure region. This is concurrent with previous data in the low-flow regions. The flow environment does not seem to be stable in these low flow regions.

In order to find the Reynolds number dependence of the discharge coefficient, the percent change in differential pressure across the slotted orifice plate portion of the Equation 17 is divided out of the equation. By taking the differential pressure out of the equation, the discharge coefficient should not vary due to compressibility effects. Instead the Reynolds number effects and any variation in the plates such as geometry are left. To determine the Reynolds number

dependence, the discharge coefficient ratio is divided by a segment of Equation 13 shown in Equation 17,

$$1 - b\left(\frac{\Delta P}{P}\right)^{c} \qquad [17]$$

Coefficient (b) was determined by finding the slope of the line in Figure 39. For the 0.430 beta slotted orifice plates this is –0.5166. The 0.467 beta slotted plate slope is equal to –0.6. Since the data forms a straight line, coefficient (c) is equal to one. The discharge coefficient is divided by Equation 17 to provide the Reynolds number dependence for the 0.430 Beta ratio slotted orifice plates as is plotted in Figure 40. Figure 40 shows that there is a Reynolds number difference. All of the three lines shown in this graph start at a discharge coefficient of one and then slope down. These lines represent the three different pressure conditions ran in this test. The high-pressure data is the bottom line. The different points for each line correspond to different flow rates. The high-pressure data produces lower discharge coefficients much more rapidly than the lower pressures. The lowest discharge coefficient produced was about 0.80.

The same method was performed for the 0.467 Beta slotted orifice plates. The discharge coefficient ratio is plotted versus the percent change in pressure across the slotted orifice plate in Figure 41. This data does not overlay as well as the 0.430 plates. The slope of this data was determined and put into Equation 17 in order to find the Reynolds number dependence of the discharge

coefficient that is plotted versus the Reynolds number as shown in Figure 42. Once again similar data is produced. The high pressure data is the bottom line of Figure 42. The discharge coefficient reaches a low point of approximately 0.75 for this data, 0.05 lower than the 0.430 slotted orifice plate.

Area Analysis Results

The slotted orifice plates with beta ratios of 0.467 and 0.430 were scanned. The Sigma Scan software program calculated the area of the slots. Flores documented that the 0.467 beta ratio plate should have a total slotted orifice area of 4.5 square centimeters (0.697 square inches). The 0.430 beta ratio plate has been documented to have a total slotted orifice area of 3.88 square centimeters (0.6 square inches). All of the plates tested in this study showed values of at least a hundredth of an inch less than the values calculated by Flores. The 0.467 beta ratio plates ranged in area from 4.34 square centimeters (0.67 square inches) to 4.41 square centimeters (0.68 square inches). The plates vary by 1.4%. This is 3-4% less than Flores's results. The beta ratio plates of 0.430 plates range in total area from 3.81 to 3.86 square centimeters (0.59 to 0.598 square inches). This is a difference of 1.3%. The values are 12.3% to 13.5% less than Flores's measurements. The graphs of the 0.467 beta ratio and 0.430 beta ratio total area scanned from each plate are shown respectively in Figures 45 and 46.

The y-intercept and area analysis show that on some plates the discharge coefficient is dependent on the manufacturing difference. However, for the 0.430 beta ratio plate that proved great repeatability, only three of 7 plates exemplify this quality. The total area of each plate was compared to the (a) coefficient. The (a) coefficient is equivalent to the y-intercept on Figures 37 and 38. This y-intercept and slotted plate area are shown in Figures 43 and 44. The 0.430 results are shown in Table 9. The 0.467 results are shown in **Table 10**. The plates are arranged in the order of increasing coefficient (a) or y-intercept. Table 9 shows that the first 4 plates analyzed of a beta ratio 0.430, number 8,3,7, and 6, have scrambled data when comparing the y-intercept and actual area of the slots. Increasing the slotted area of the plates does not increase the (a) coefficient. However the last three 0.467 beta ratio plates, 2,1 and 4 have a coefficient (a) or y-intercepts and area that both increase in ascending order. Table 10 shows that the smallest coefficient (a) and area is plate 9. Plate 7 is next that has increasing coefficient (a) and area then plates 2 and 4 reverse the coefficient (a) and area. The individual slot areas of each plate for the 0.430 beta ratio slotted plates are shown Figures 47 through 56. The individual slot areas of each plate for the 0.467 beta ratio slotted plates are shown in Figures 57 through 63. The charts for this data are respectively in Table 11 and 12 for the 0.467 and 0.430 slotted orifice plates.

CONCLUSIONS

The water and air flow visualization study shows that the slotted orifice plate mixes the two-phase flow better than the standard orifice plate and V-Cone. Regardless as to whether the upstream flow conditions were stratified or annular, the mixture downstream of the slotted orifice plate mixed in all directions of the pipe. The standard orifice plate did not create the uniform, turbulent mixing as was displayed in the slotted orifice plate. Instead the two-phase mixture creates pulses that enter and exit the plate. This causes partial mixing at the lower flow conditions. At the higher flow rates, such as 0.020 m^3/s (50 cfm) there was not as much turbulence in the mixture downstream of the plate as the slotted orifice plate revealed. The V-Cone showed less mixing than the slotted and standard orifice plates. Especially at low flow rates, the two-phase mixture remains stratified downstream of the V-Cone. As the flow rate increases, the water pulses through the V-Cone creating a non-consistent mixture throughout the pipe that shows heavy streaks of water in only certain areas that flow linearly along the side of the pipe.

The oil and air visualization study measured the differential pressure across the slotted and standard orifice plates. The slotted orifice plate read a higher

differential pressure reading than the standard orifice plate due to the fact that the beta ratio for the slotted plate was lower at 0.430 rather than the 0.500 beta ratio of the standard orifice plate. The slotted orifice plate decreased by approximately 400 Pa in the first ten minutes, whereas the standard orifice plate increased by 55 Pa in the first ten minutes. The standard orifice plate differential pressure stayed fairly constant at a value of 5915 Pa. It increased and decreased by about 10 Pa throughout the test. The slotted orifice plate varied quite a bit more, approximately 200 Pa throughout the test. The discharge coefficient for the slotted orifice plate was higher than the standard orifice plate, due to the smaller beta ratios that inversely affects the discharge coefficient.

There is scatter in the low Reynolds number region, around 100,000, of the manufacturing repeatability test. This has also been evident in previous studies. There is a Reynolds number dependence on the discharge coefficient. The high-pressure data results in a lower discharge coefficient and as the flow rate is varied, it decreased at a much faster rate toward the 0.80 for the 0.467 plates or 0.75 for the 0.430 slotted orifice plate. The 0.430 slotted orifice plates produced higher reproducibility among the plates than the 0.467 slotted orifice plates. As slot area increases, the differential pressure across the plate goes down while the discharge coefficient goes up. The 0.430 coefficient (a) does vary accordingly with a larger area. As the slot area increases, the (a) coefficient

increases. The (a) coefficient is therefore dependent on the geometry of the plates.

RECOMMENDATIONS

The water and air study showed the slotted orifice plate creates more mixing and turbulence than the slotted orifice plate and V-Cone. The V-Cone showed the least amount of mixing, especially the lower flow rates where the flow remains stratified. Therefore if mixing of a two-phase flow is essential to a future study, then the slotted orifice plate will provide better results than the standard orifice plate or V-Cone.

The oil and air study showed that the slotted and standard orifice plates have opposite effects in the first ten minutes of testing before steady state is achieved. The slotted orifice plate discharge coefficient actually increases throughout the whole test while the standard orifice plate discharge coefficient decreased before it leveled out to a constant value. The slotted orifice plate may actually be better suited for oil than the standard orifice plate. This could be investigated in further studies while comparing standard and slotted orifice plates with the same beta ratio to ensure that is the reason for the differential pressure difference.

As the slot area increases, the discharge coefficient increases. Therefore, in order for slotted orifice plates to be reproducible, the plates should have tight manufacturing standards. The low Reynolds number flow conditions produced lower discharge coefficients. The low flow conditions around a Reynolds number of 100,000 shows a lot of scatter in the graphs. More sensitive turbine meter equipment should be used in the low flow regions in order to create more precise results. The 0.430 beta ratio plates provide a more stable environment in these low differential pressure regions. It also provided more reproducible data than the 0.467 plates. Therefore, any further studies involving the slotted orifice plate should include the 0.430 beta ratio plate.

REFERENCES

[1] Morrison, G.L., Hall, K.R., Holste, J.C., DeOtte, R.E., Jr., Macek, M.L. and Ihfe, L.M., 1994, “Slotted Orifice Flowmeter,” AlChE Journal, Vol.40, No.10, pp. 1757-1760.

[2] Morrison, G.L., Hall, K.R., Holste, J.C., Macek, M.L., Ihfe, L.M., DeOtte, R.E., Jr., and Terracina, D.P., 1995, “Slotted Comparison of Orifice and Slotted Plate Flowmeters,” Flow Measurement and Instrumentation, Vol. 5, No. 2, pp. 71-77.

[3] M.L. Ihfe, Development of Slotted Orifice Flow Conditioner, M.S. Thesis, Texas A&M University, College Station, TX, 1994.

[4] Terracina, D.P., The Experimental and Numerical Developments of a Slotted Orifice Meter and its Design parameters, Ph.D. Dissertation, Texas A&M University, College Station, TX, 1996.

[5] Morrison, G.L., Hall, K.R., Macek, M.L., Ihfe, L.M., DeOtte, R.E., Jr., and Hauglie, J.E., 1994, “Upstream Velocity Profile Effects On Orifice

Flowmeters," Flow Measurement and Instrumentation, Vol. 5, No. 2, pp. 87-92.

[6] Flores, A.E., Evaluation of a Slotted Orifice Plate Flow Meter Using Horizontal Two Phase Flow, M.S. Thesis, Texas A&M University, College Station, TX, 2000.

[7] Morrison, G.L., Hall, K.R., Holste, J.C., Macek, M.L., Ihfe, L.M., DeOtte, Jr. R.E., Terracina, D.P.,1994, "Comparison of Orifice and Slotted Plate Flowmeters," Flow Measurement and Instrumentation, pp. 71-74.

[8] Hall, K.R, Morrison, G.L., 2000, "Slotted Orifice Flow Meter," AICHE Inst Meeting.

[9] Macek, M.L., A Slotted Orifice Plate Used as a Flow Measurement Device, M. S. Thesis, Texas A&M University, College Station, TX, 1993.

[10] Brewer, C.V., Evaluation of the Slotted Orifice Plate as a Two-Phase Flow Meter, M.S. Thesis, Texas A&M University, College Station, TX, 1999.

[11] Brewer, C.V., Flores, A., Hall, K.R., Morrison, G.L., 2002, “Universal Slotted Orifice Flow Meter Flow Coefficient Equation for Single and Two Phase Flow,” 5th Int. Flow Symposium.

[12] Muralidharan, V., Response of a Slotted Plate Flow Meter to Horizontal Two Phase Flow, M.S. Thesis, Texas A&M University, College Station, TX, 2003.

.

APPENDIX A

FIGURES

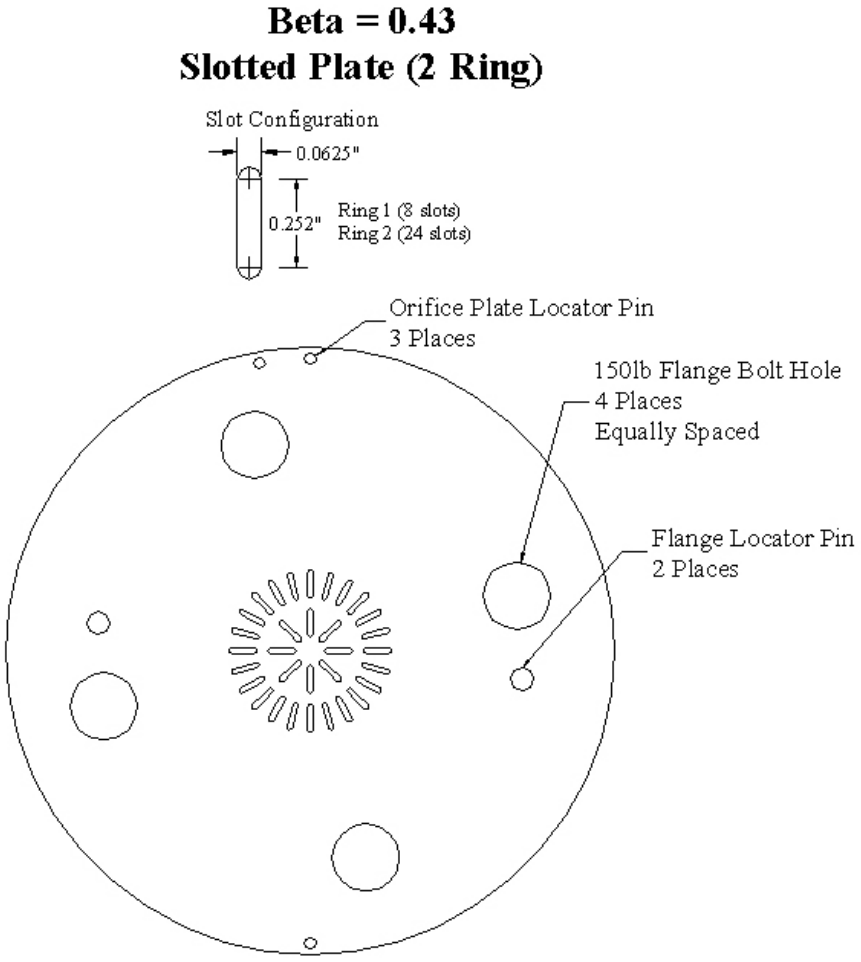

Figure 1: 0.430 Beta Slotted Plate

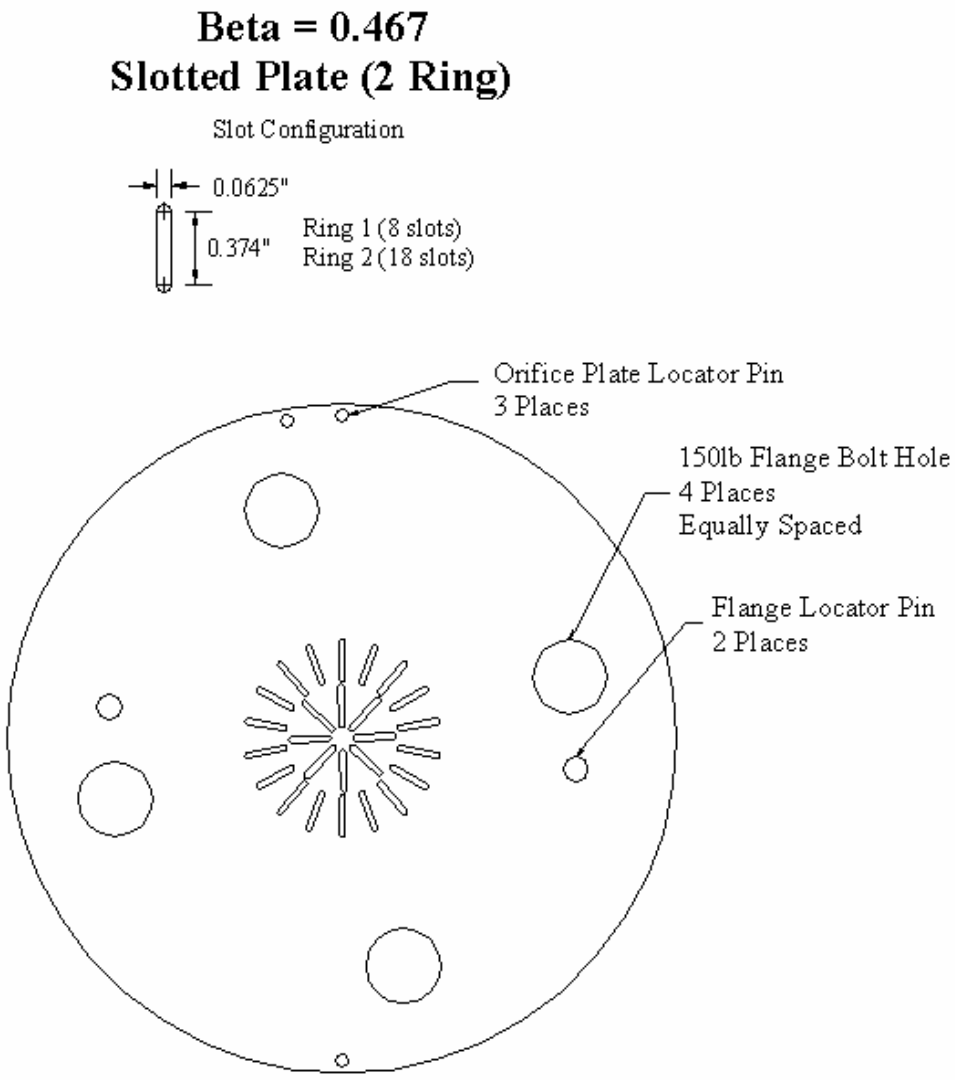

Figure 2: 0.467 Beta Slotted Plate

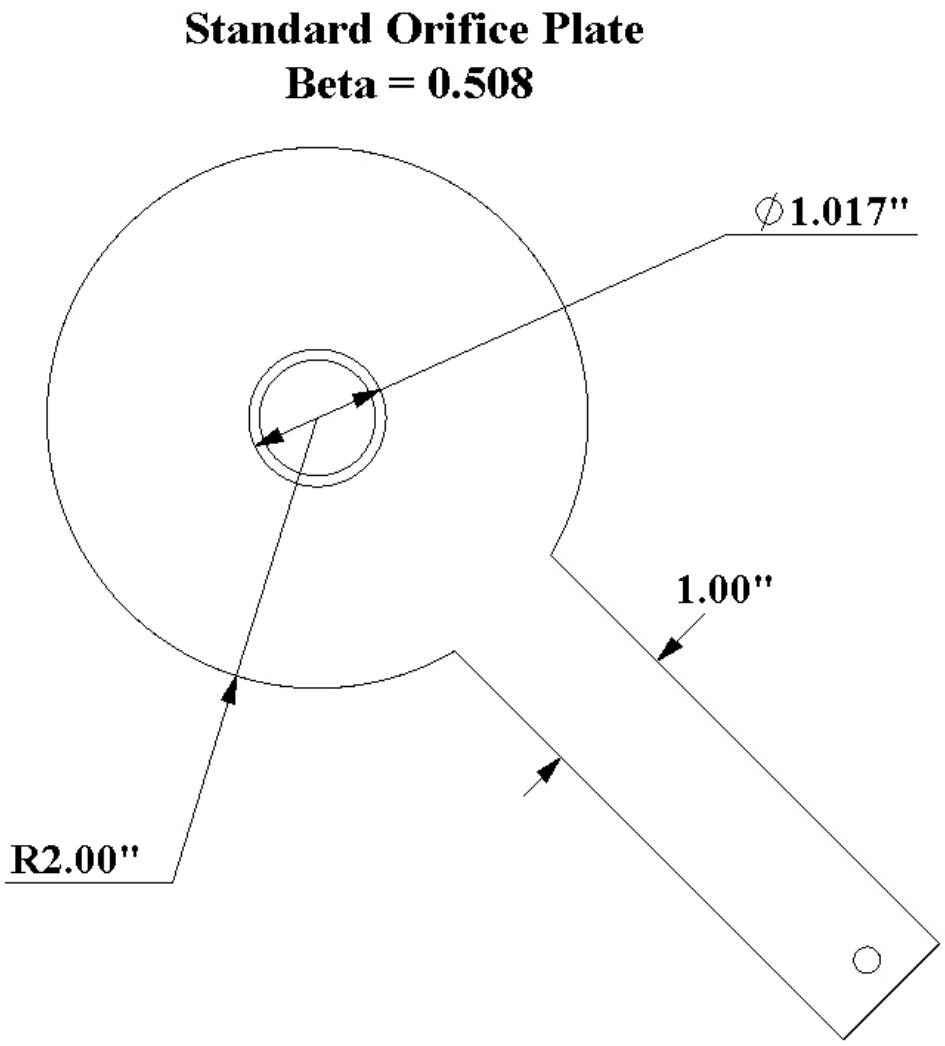

Figure 3: Standard Orifice Plate

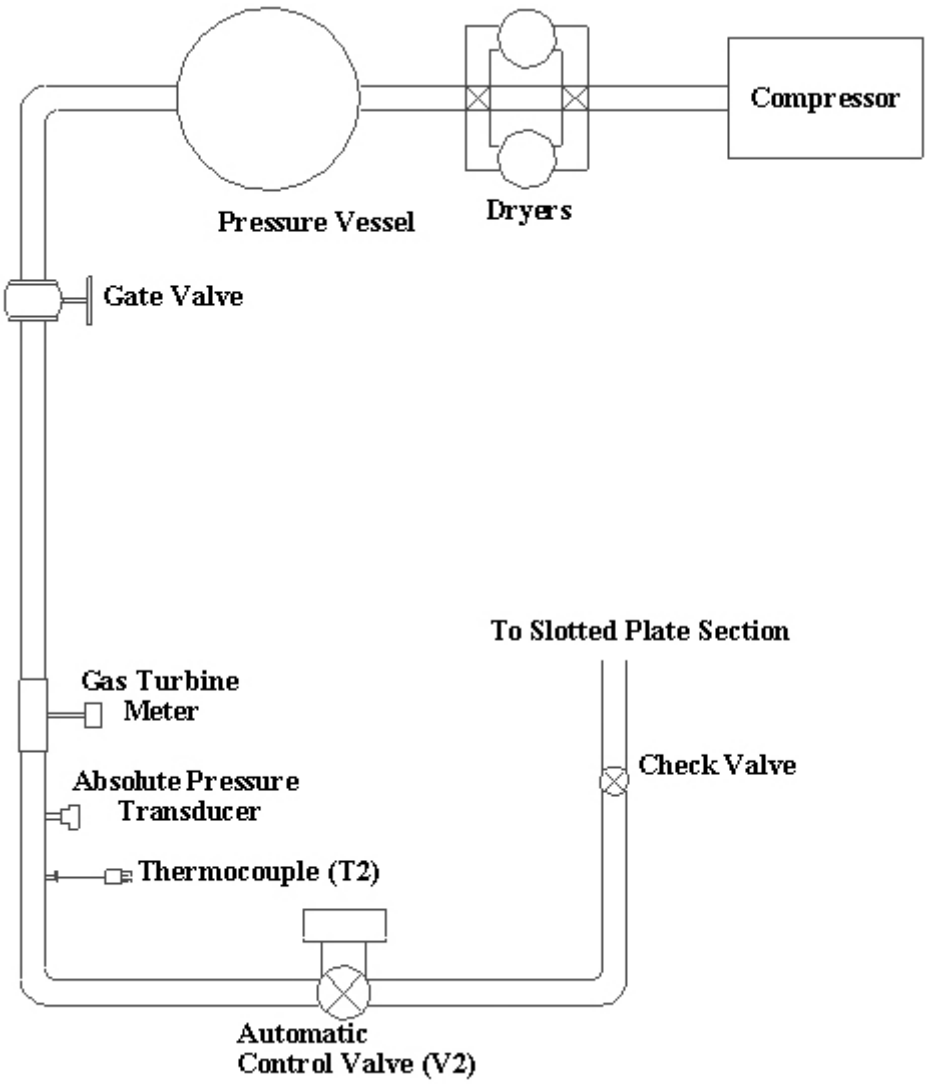

Figure 4: Air Metering Section

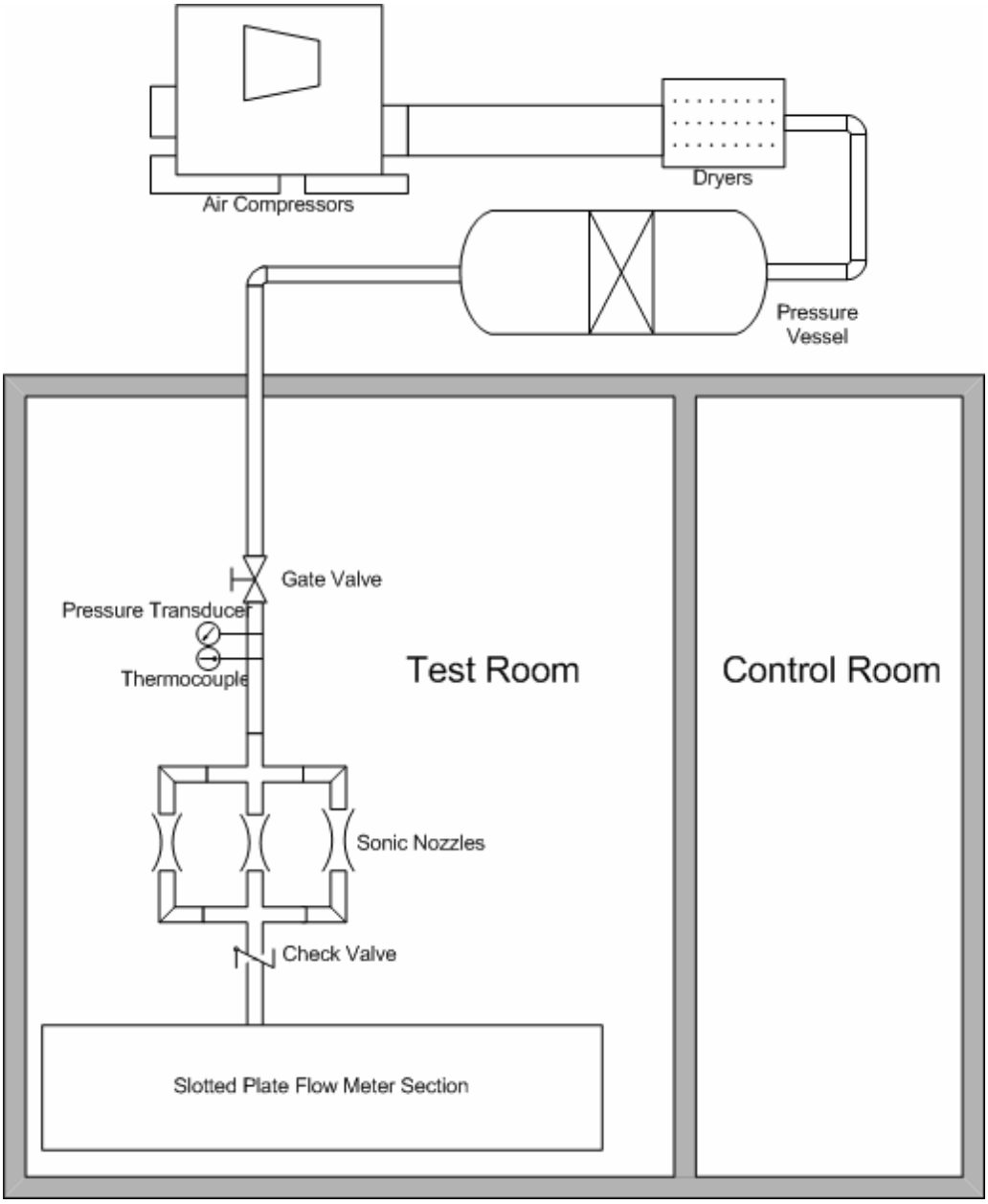

Figure 5: Sonic Nozzle Bank Air Metering Section

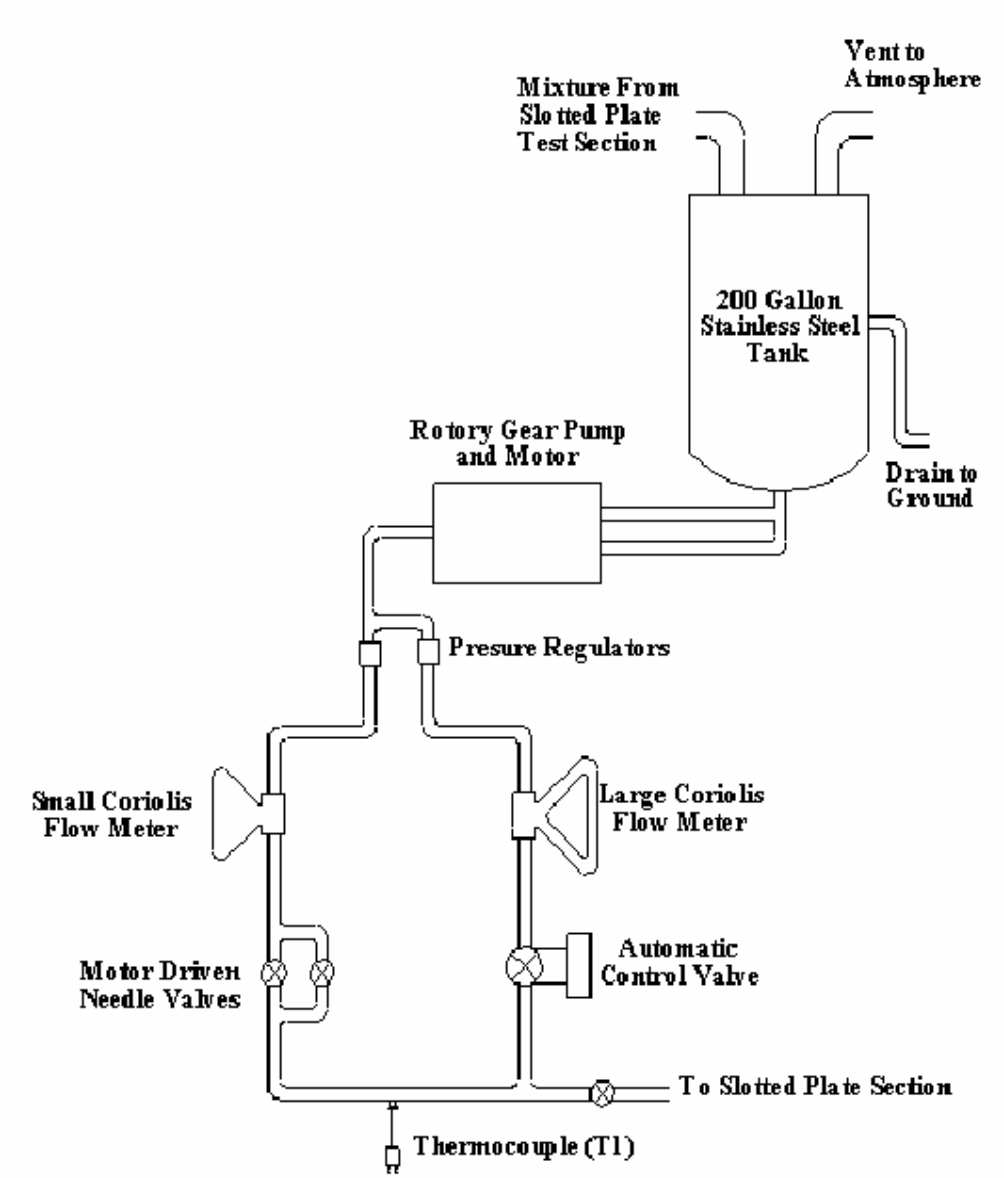

Figure 6: Water Metering Section

Figure 7: 0.009 m^3/s 90% Quality

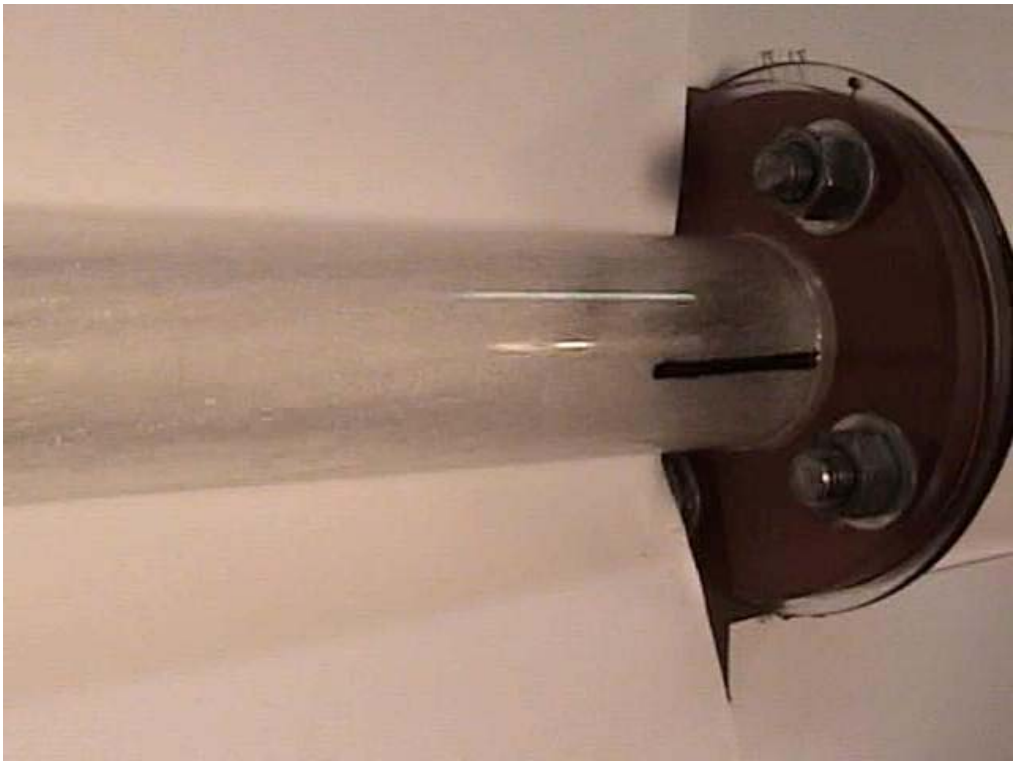

Figure 8: 0.009 m^3/s 90% Quality Downstream

Figure 9: 0.009 m^3/s 40% Quality

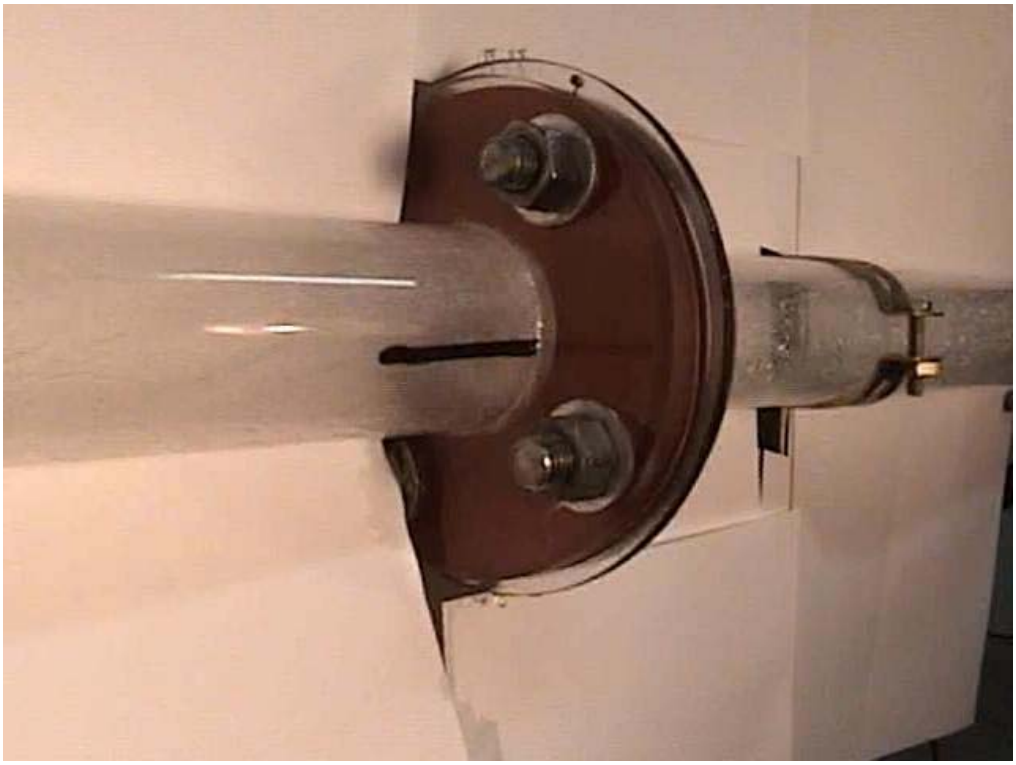

Figure 10: 0.009 m^3/s 40% Quality Downstream

Figure 11: 0.009 m^3/s 20% Quality

Figure 12: 0.02 m^3/s 90% Quality

Figure 13: 0.020 m^3/s 90% Quality Downstream

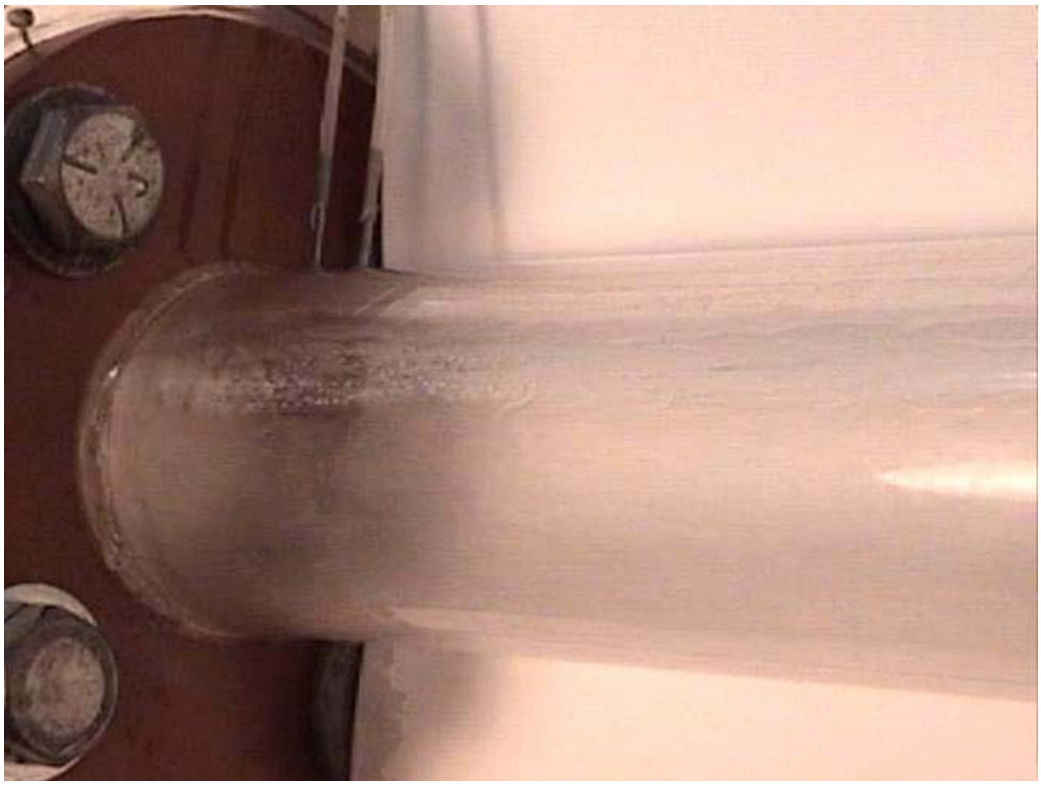

Figure 14: 0.020 m^3/s 60% Quality

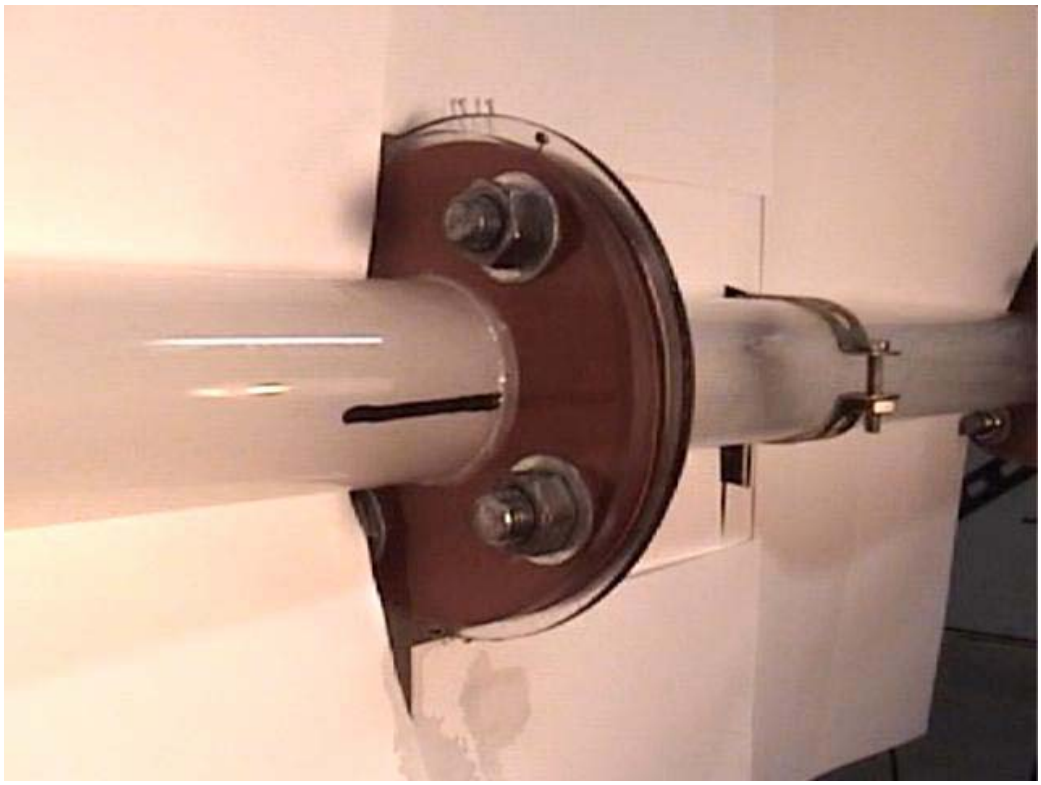

Figure 15: 0.020 m^3/s 60% Quality Downstream

Figure 16: 0.020 m^3/s 50% Quality Downstream

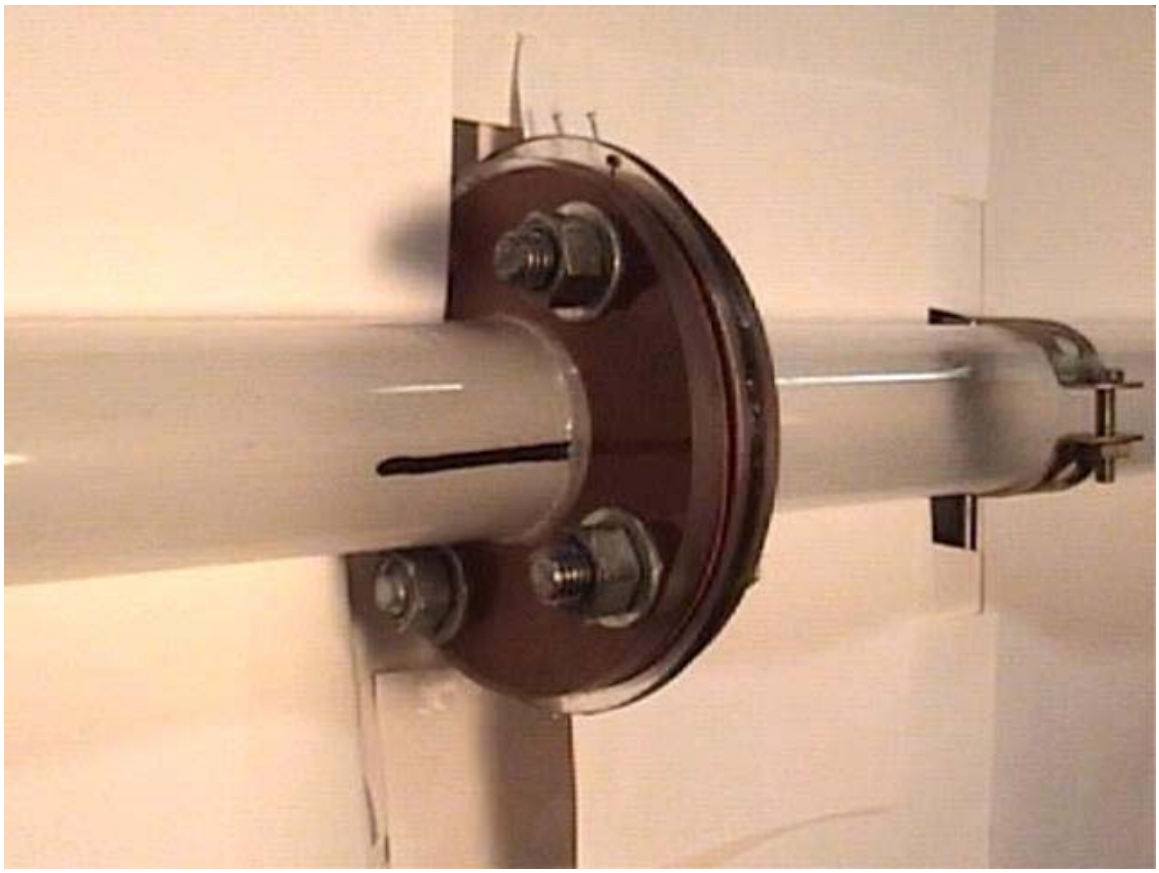

Figure 17: 0.030 m^3/s 80% Quality

Figure 18: 0.030 m^3/s 80% Downstream

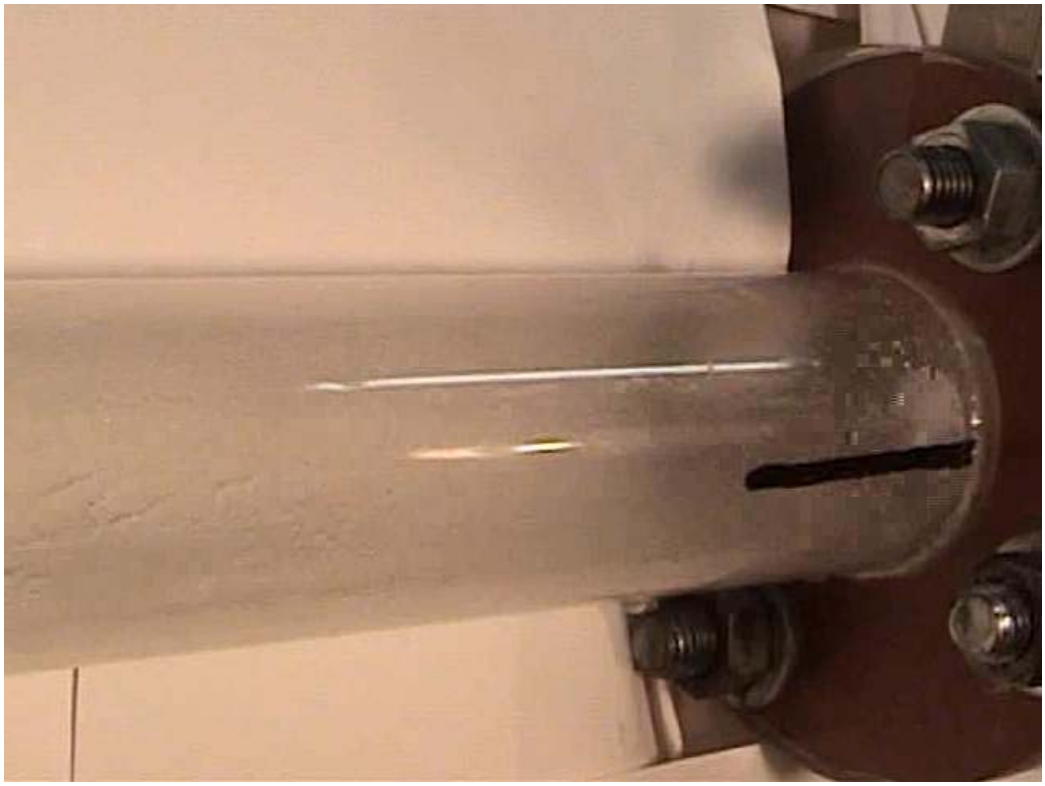

Figure 19: Standard 0.009 m^3/s 90% Quality Downstream

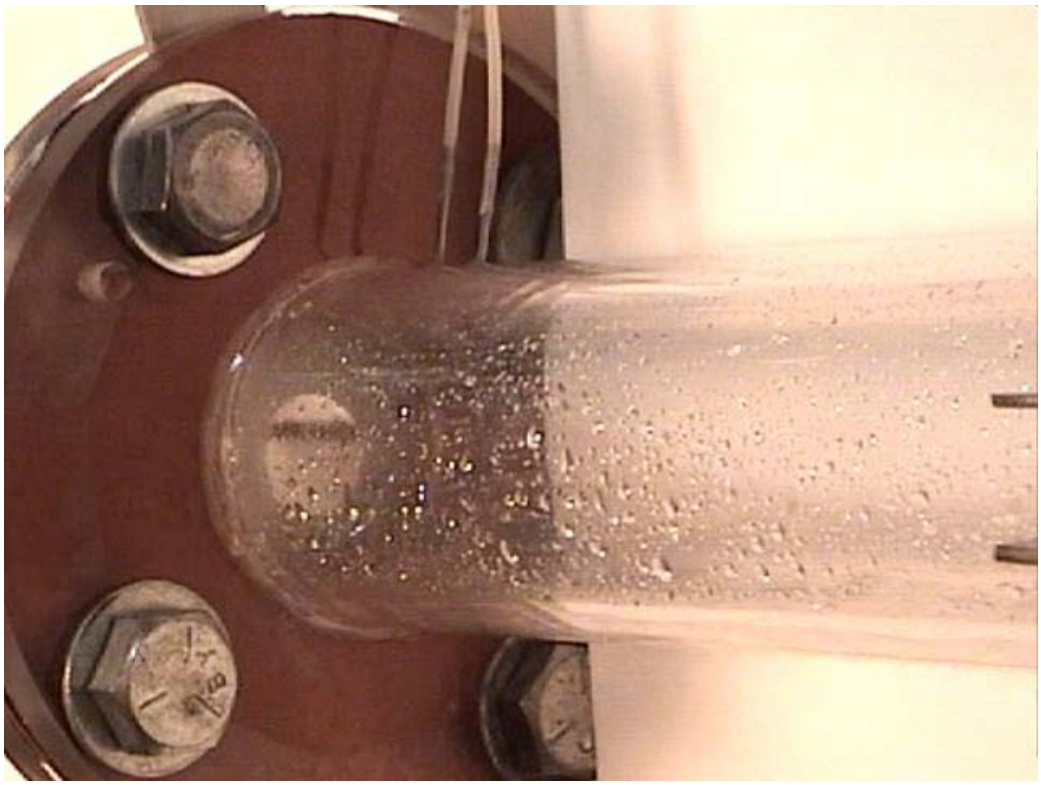

Figure 20: Standard 0.009 m^3/s 70% Quality

Figure 21: Standard 0.009 m^3/s 70% Quality Downstream

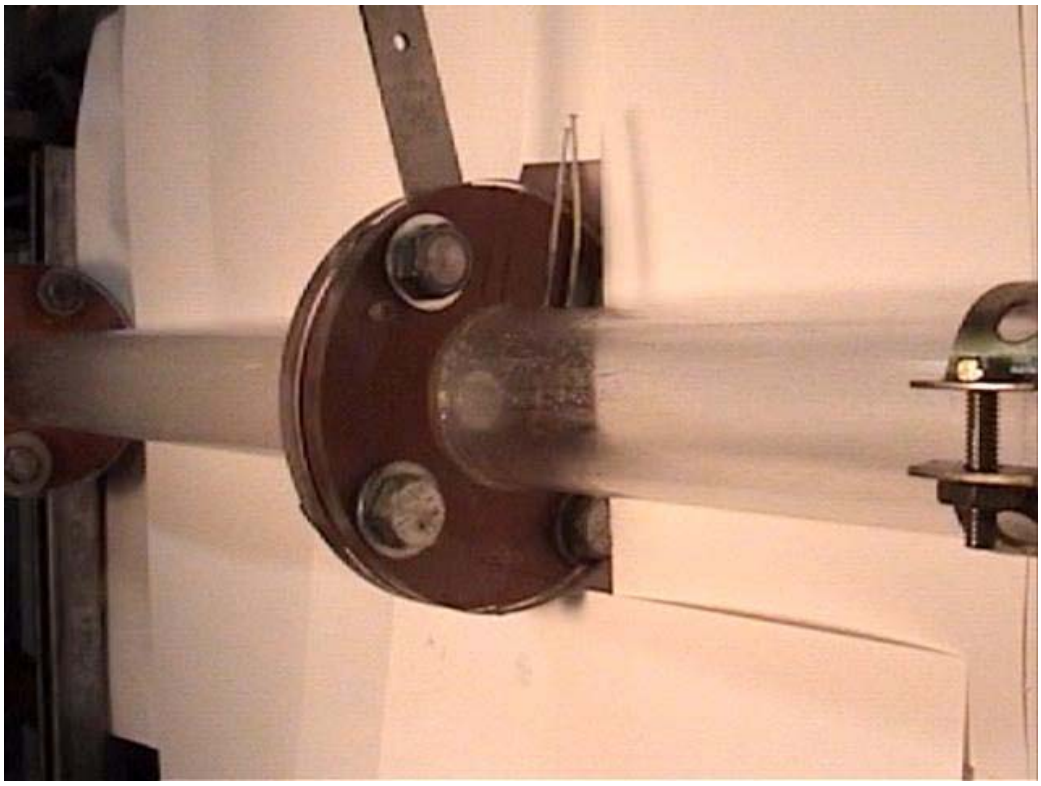

Figure 22: Standard 0.020 m^3/s 90% Quality

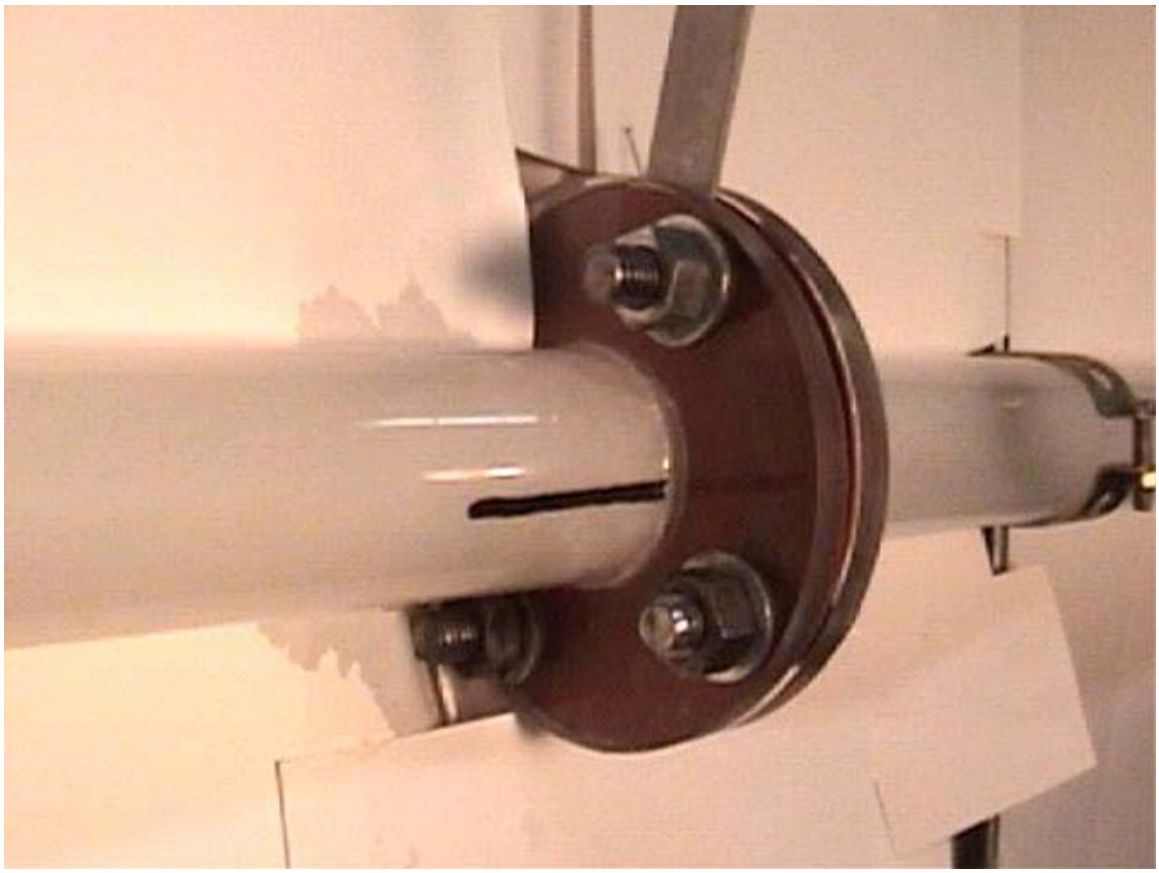

Figure 23: Standard 0.020 m^3/s 40% Quality

Figure 24: Standard 0.030 m^3/s 90% Quality

Figure 25: Standard 0.030 m^3/s 70% Quality

Figure 26: V-Cone 0.009 m^3/s 90% Quality

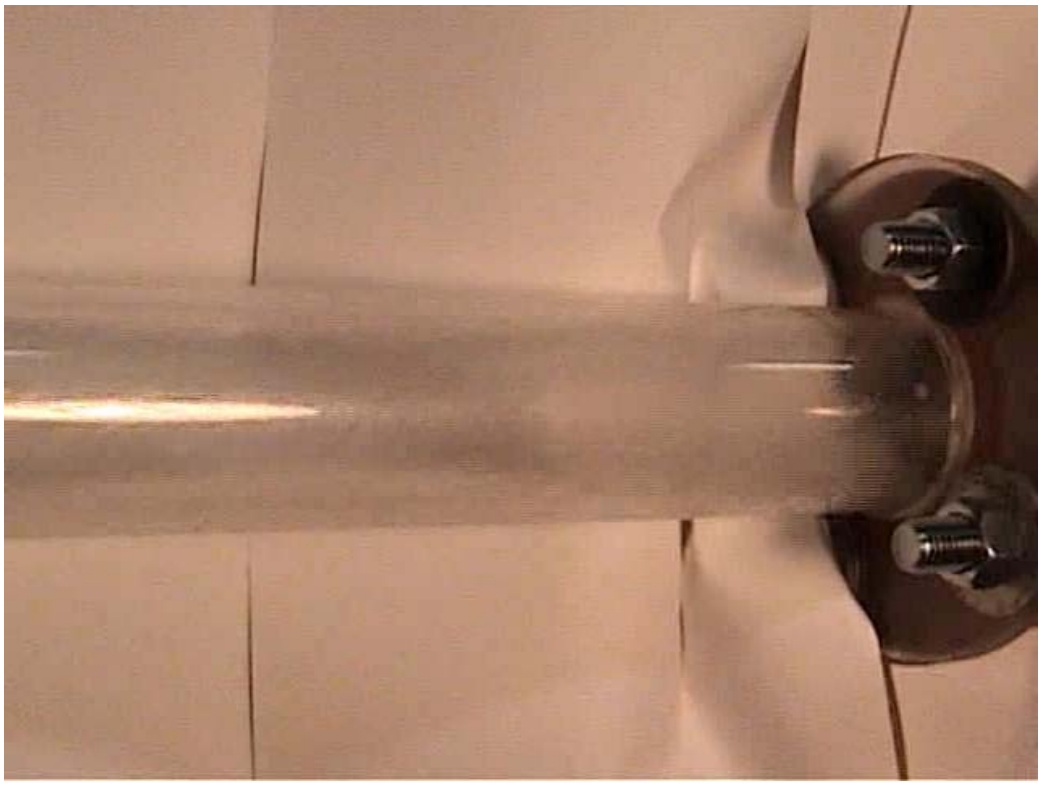

Figure 27: V-Cone 0.009 m^3/s 50% Quality

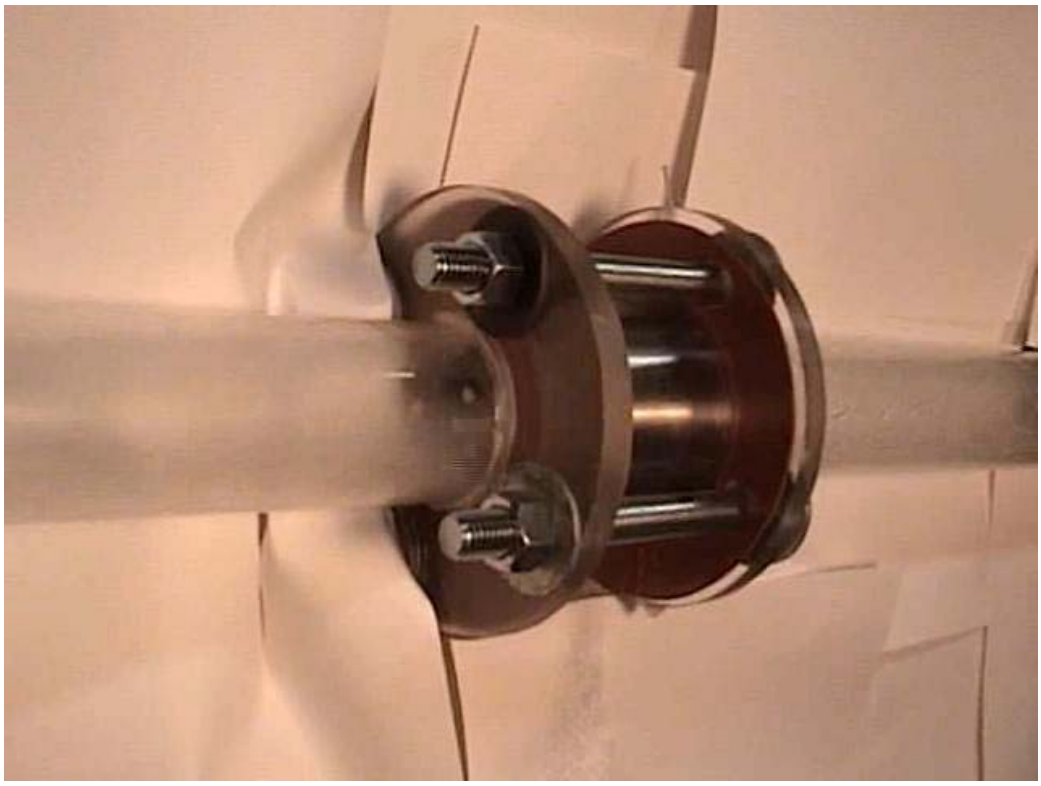

Figure 28: V-Cone 0.009 m^3/s 30% Quality

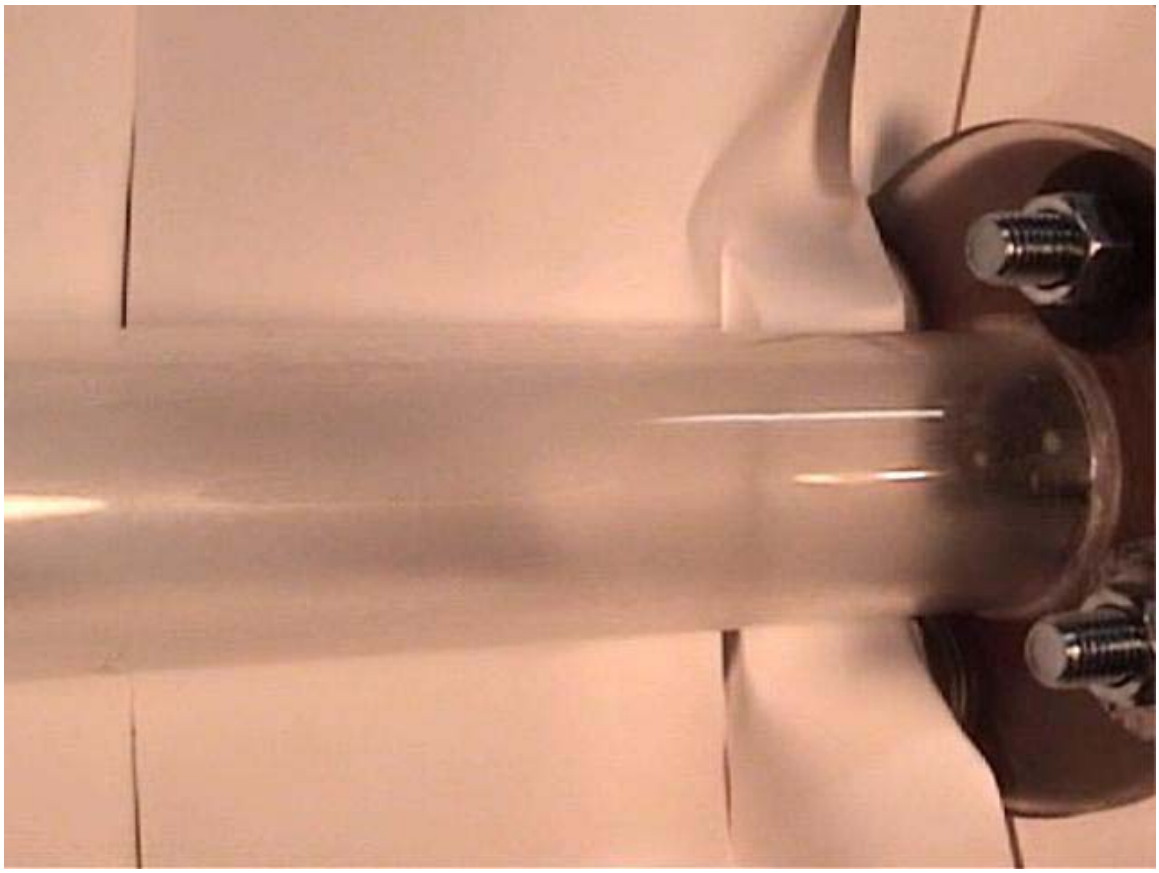

Figure 29: V-Cone 0.020 m^3/s 90% Quality

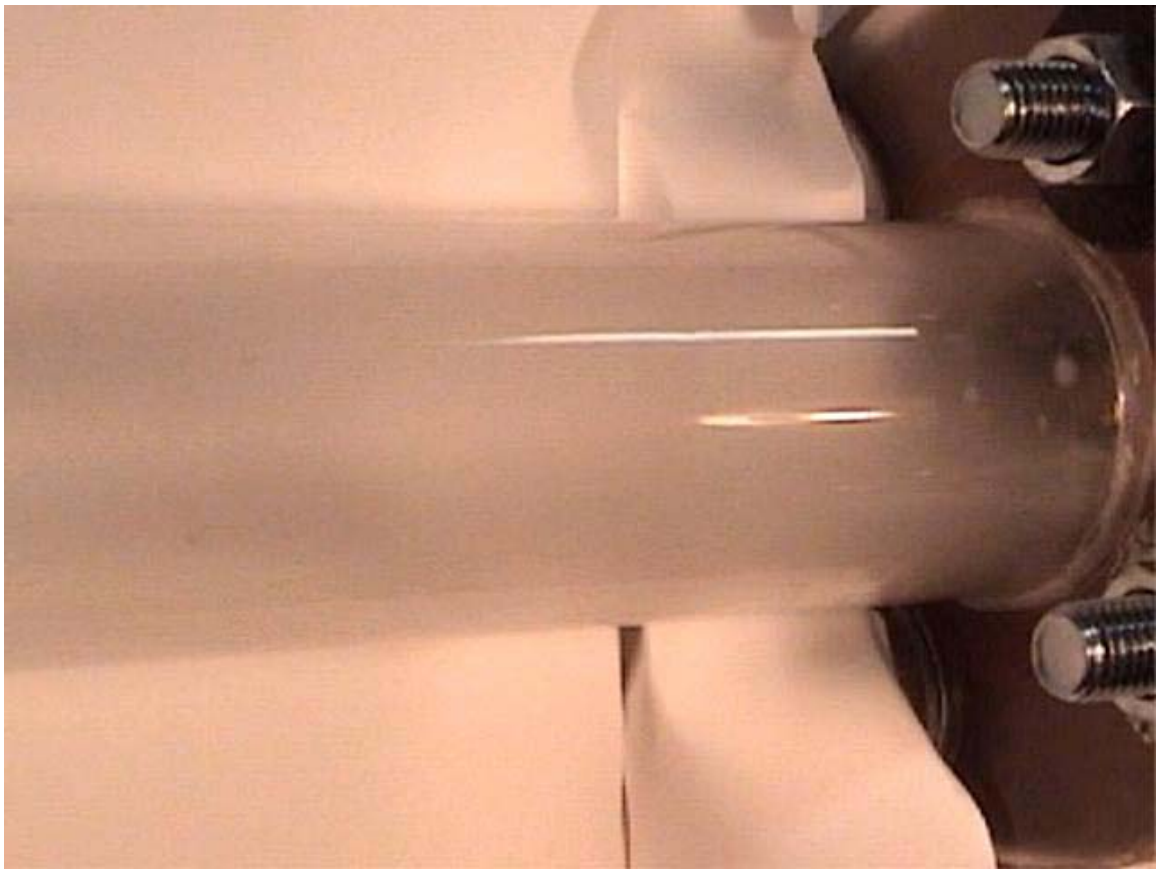

Figure 30: V-Cone 0.020 m^3/s 70% Quality

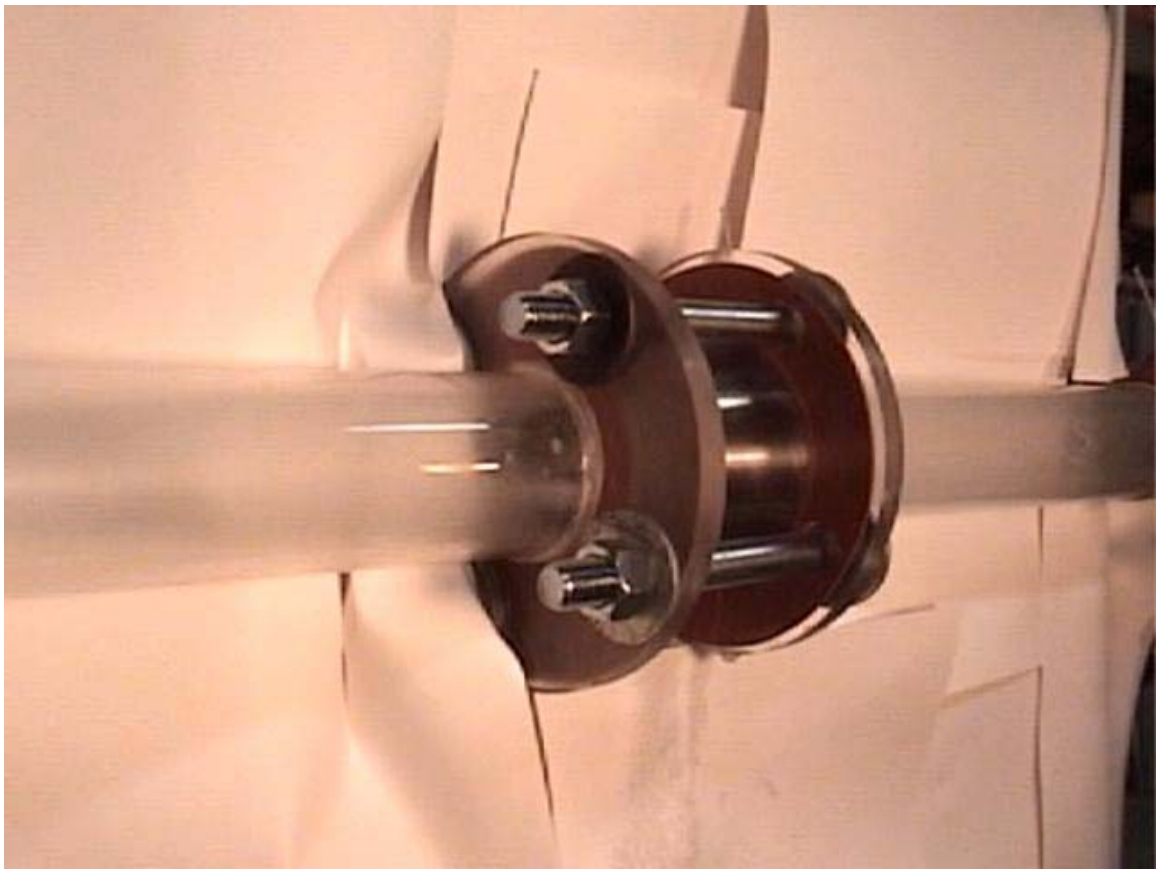

Figure 31: V-Cone 0.030 m^3/s 90% Quality

Figure 32: Oil Visualization Video Clip

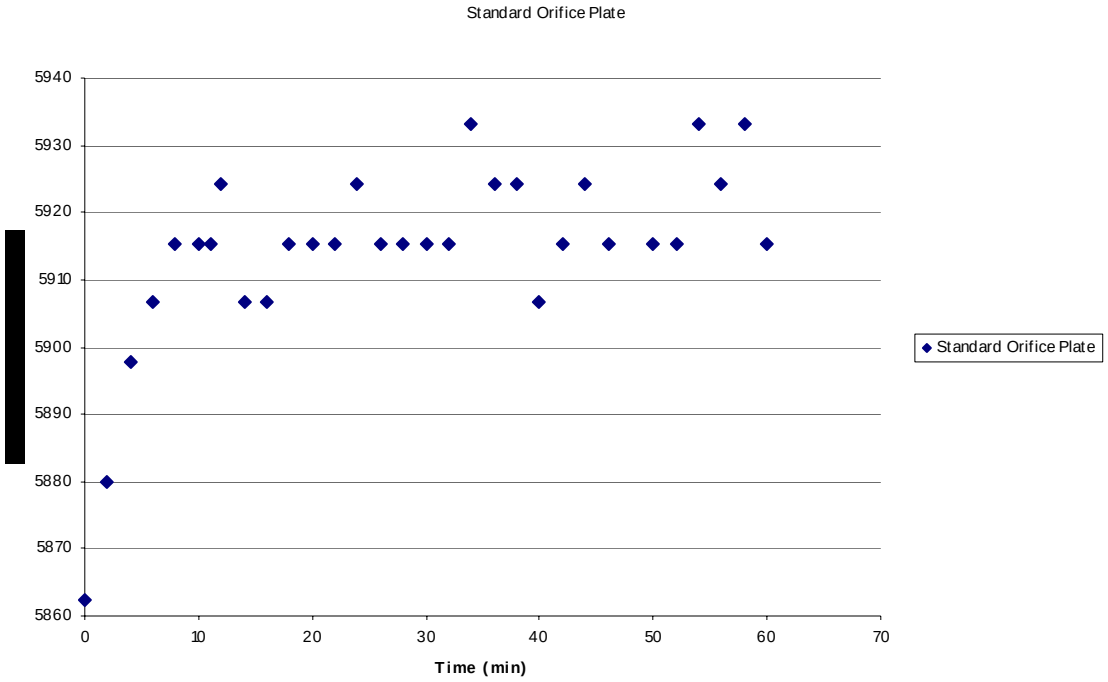

Figure 33: Standard Orifice Plate Differential Pressure

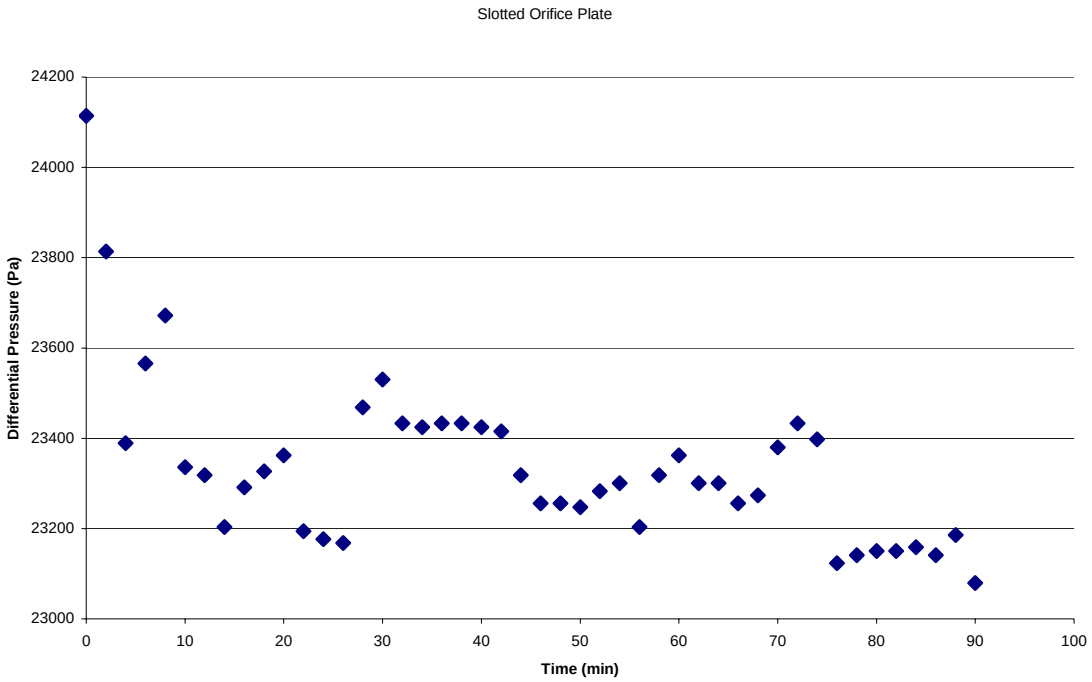

Figure 34: Slotted Orifice Plate Differential Pressure

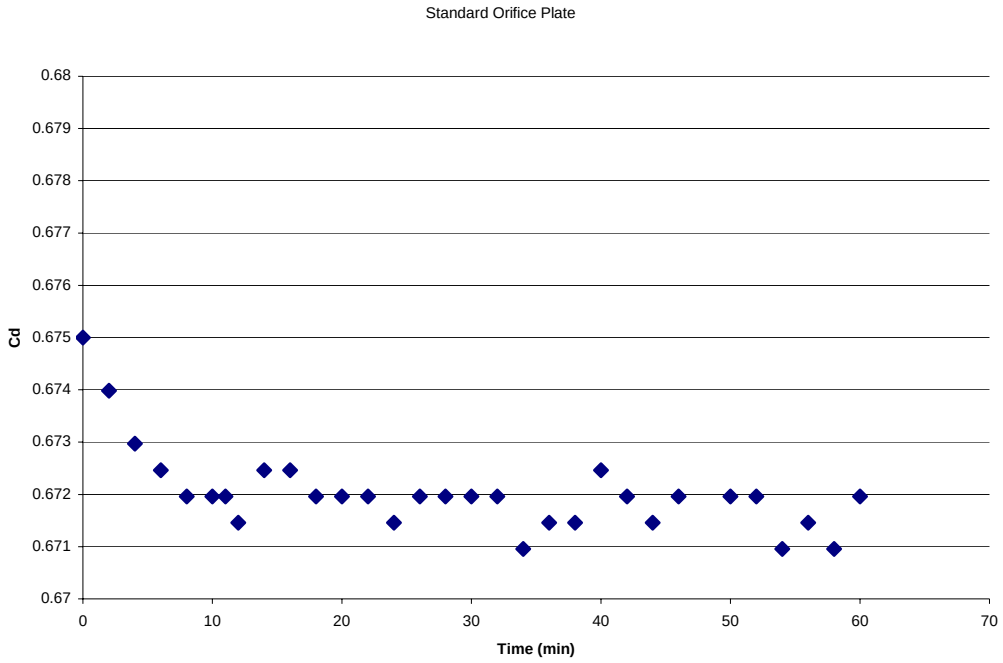

Figure 35: Standard Orifice Plate Oil/Air C_d

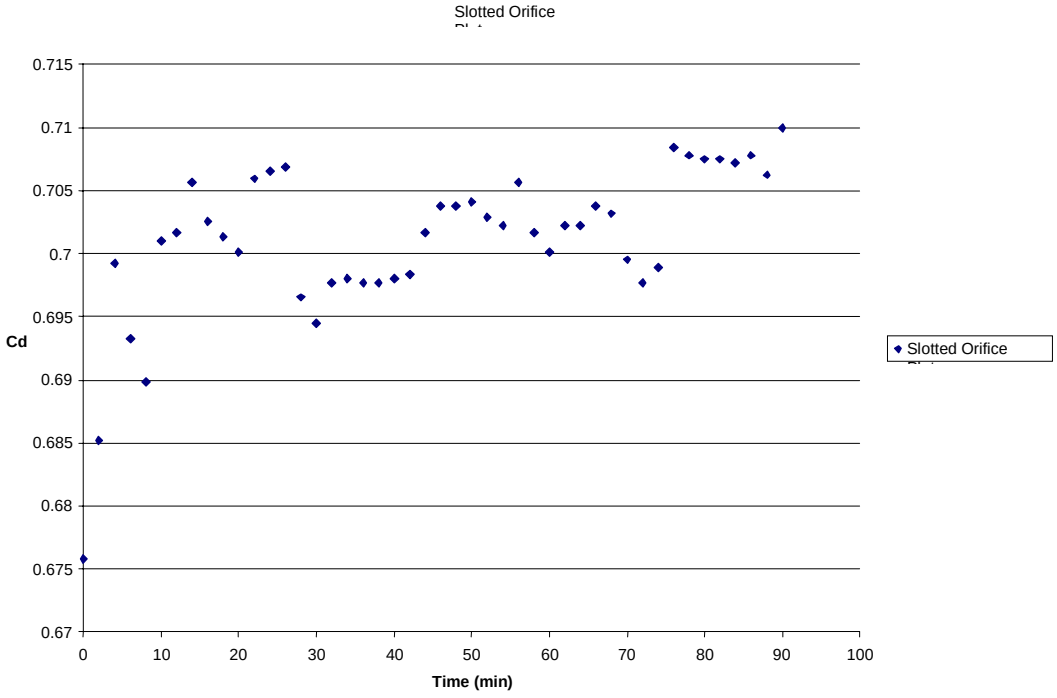

Figure 36: Slotted Orifice Plate Oil/Air C_d

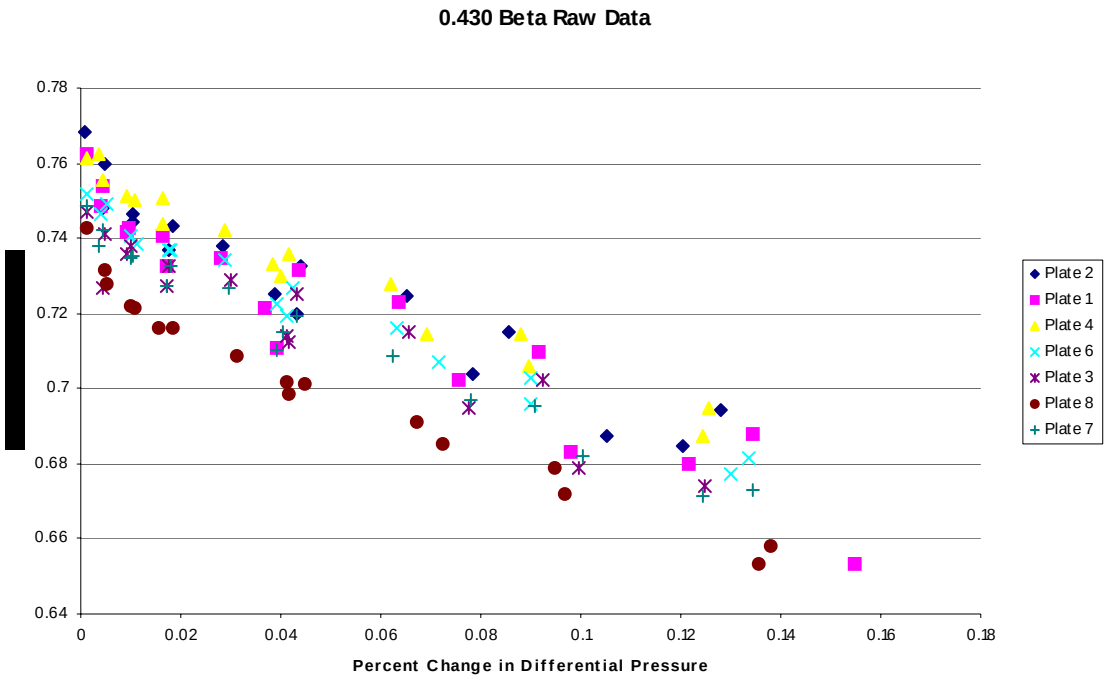

Figure 37: 0.430 Beta Raw Data

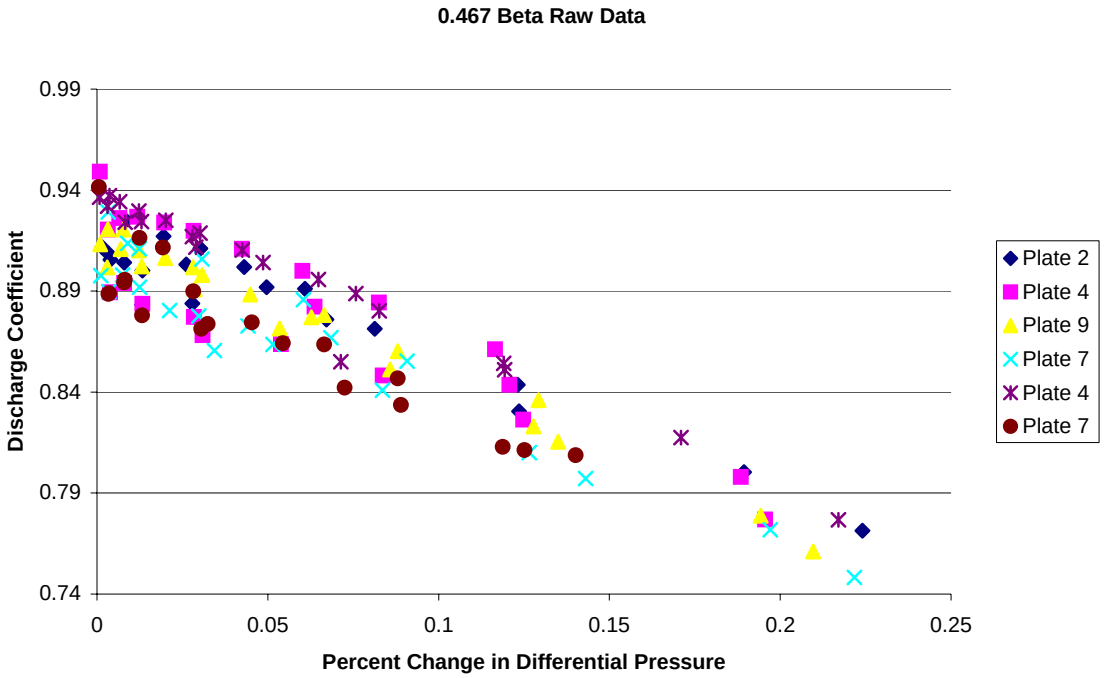

Figure 38: 0.467 Beta Raw Data

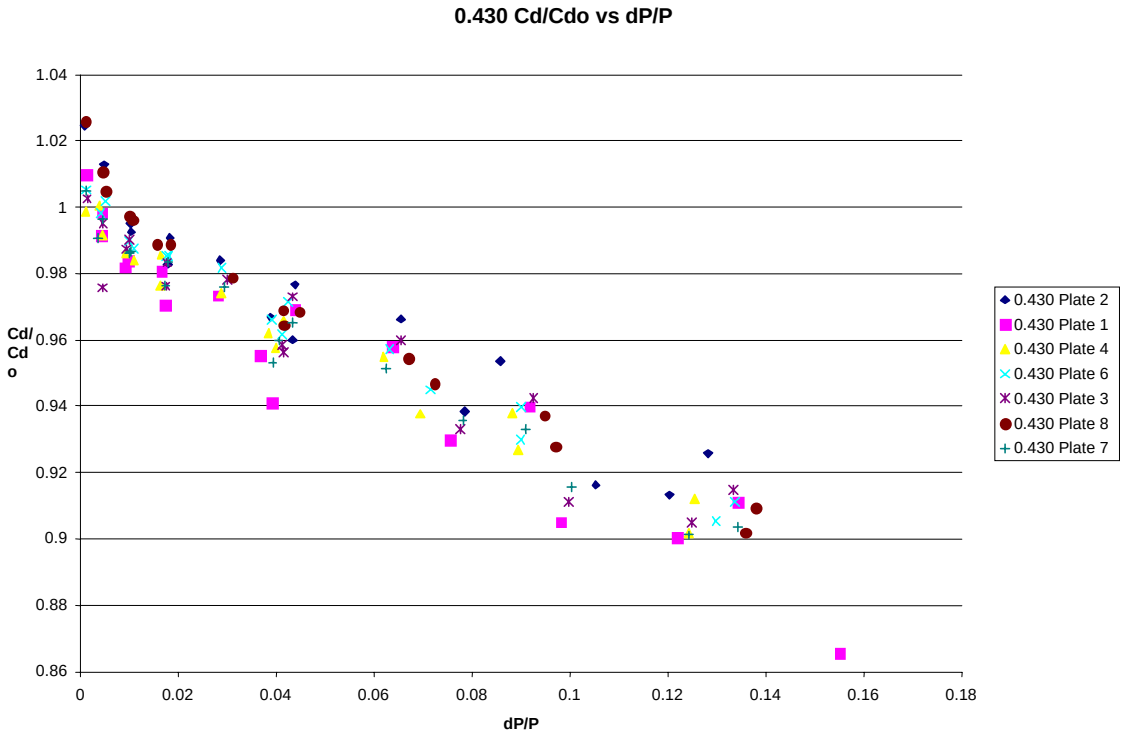

Figure 39: Beta 0.430 Discharge Coefficient Ratio

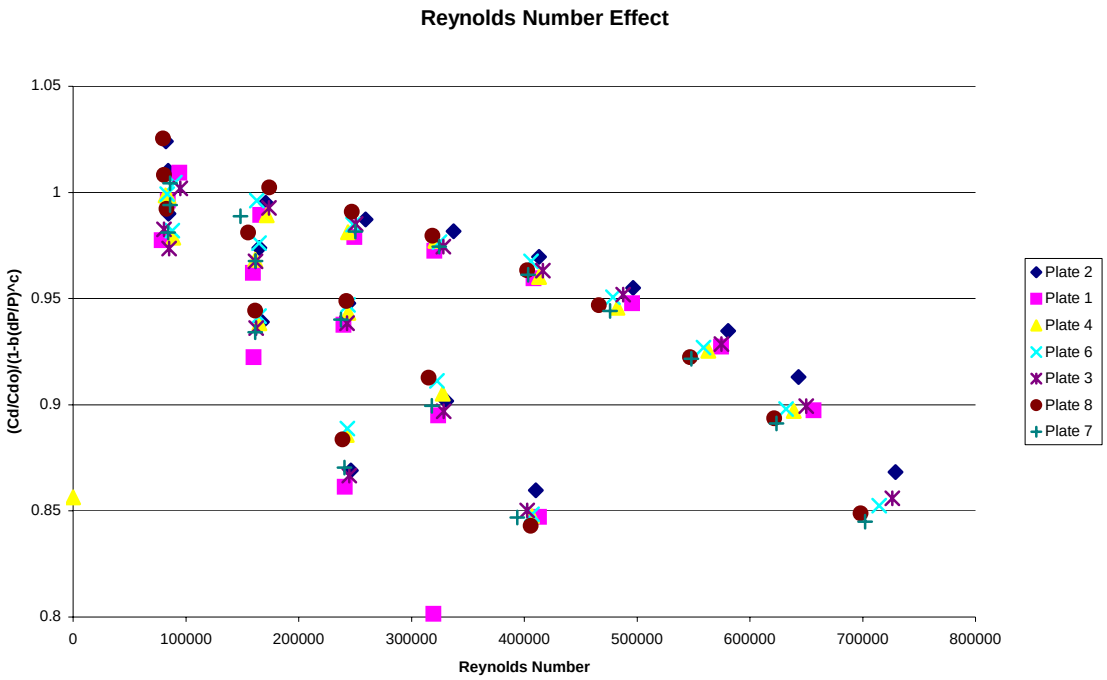

Figure 40: 0.430 Beta Reynolds Number Dependence

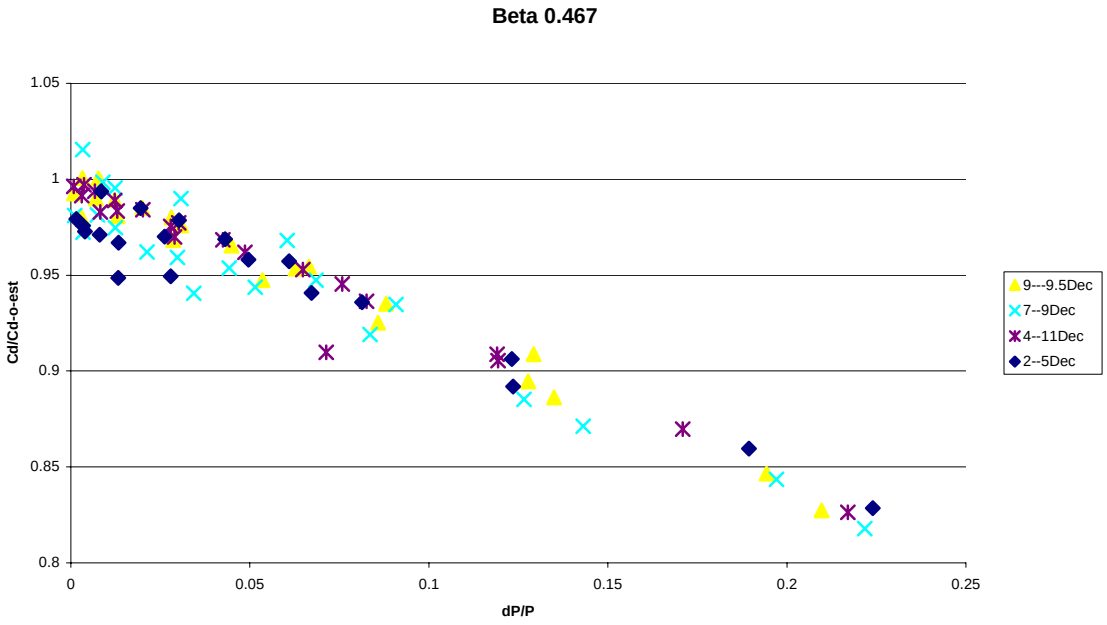

Figure 41: Beta 0.467 Discharge Coefficient Ratio

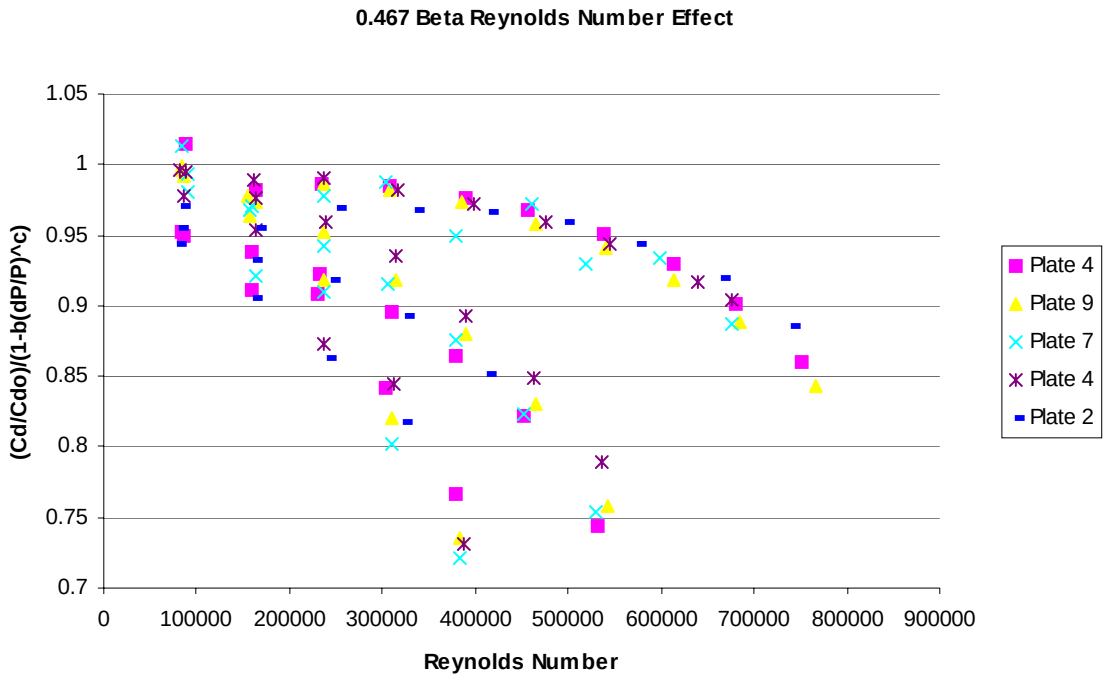

Figure 42: 0.467 Beta Reynolds Number Dependence

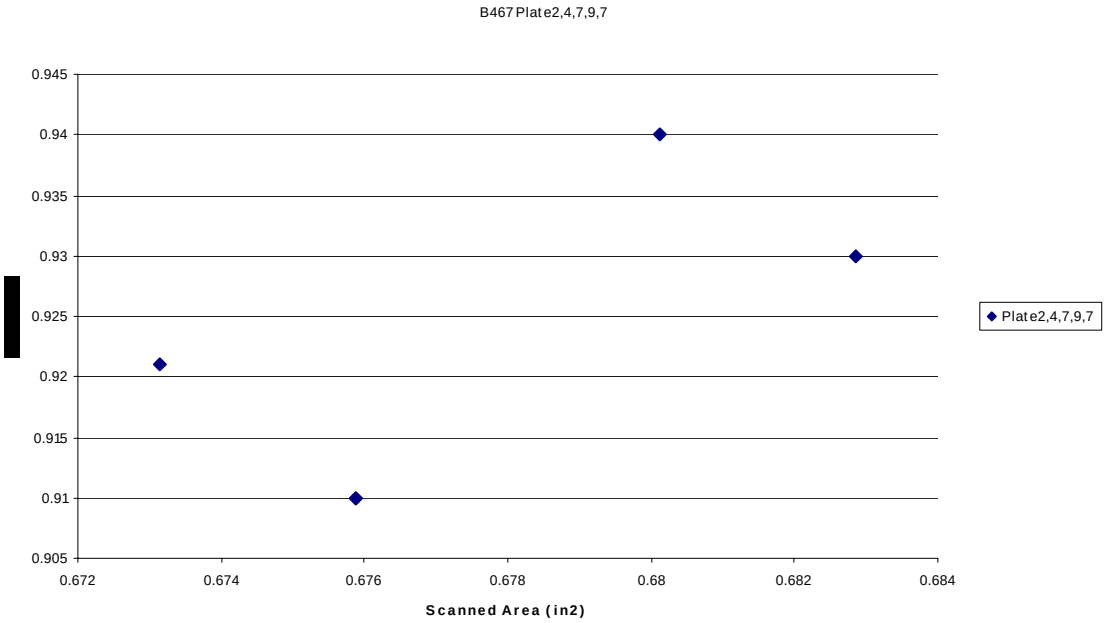

Figure 43: Beta 0.467 Intercepts vs. Area

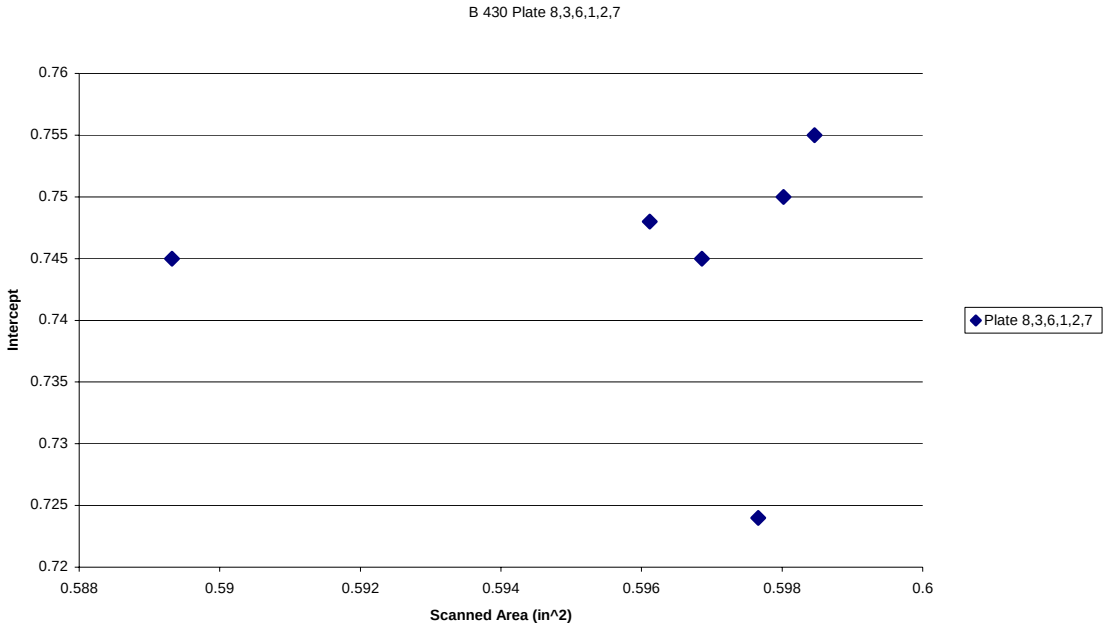

Figure 44: Beta 0.430 Intercepts vs. Area

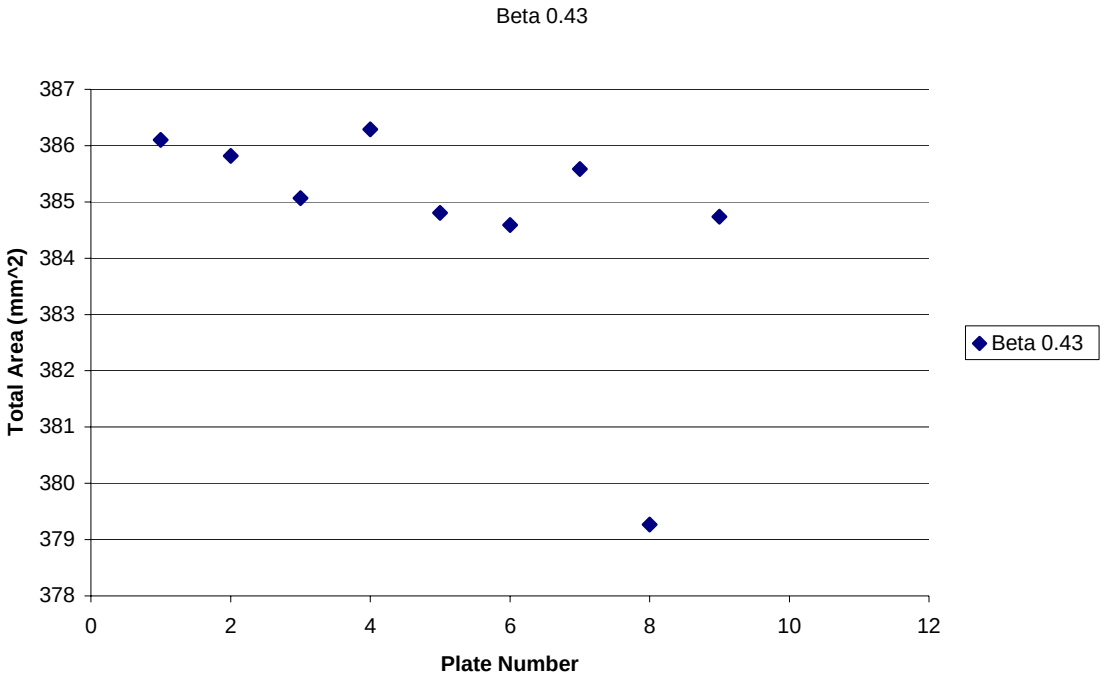

Figure 45: 0.430 Beta Total Area Scanned

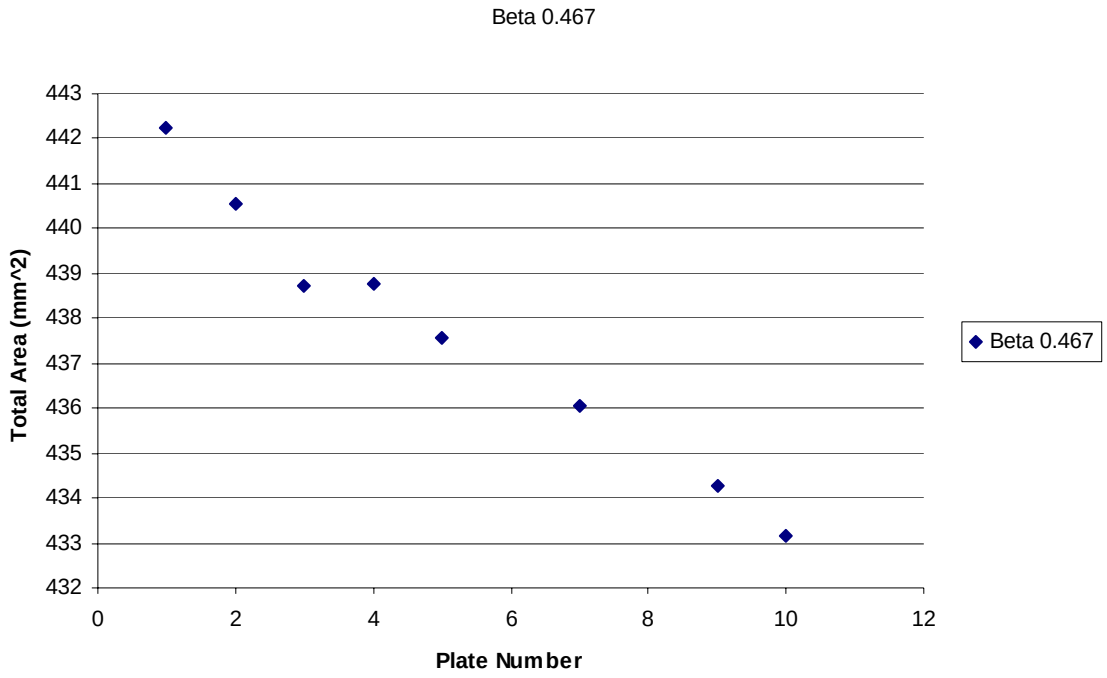

Figure 46: 0.467 Beta Total Area Scanned

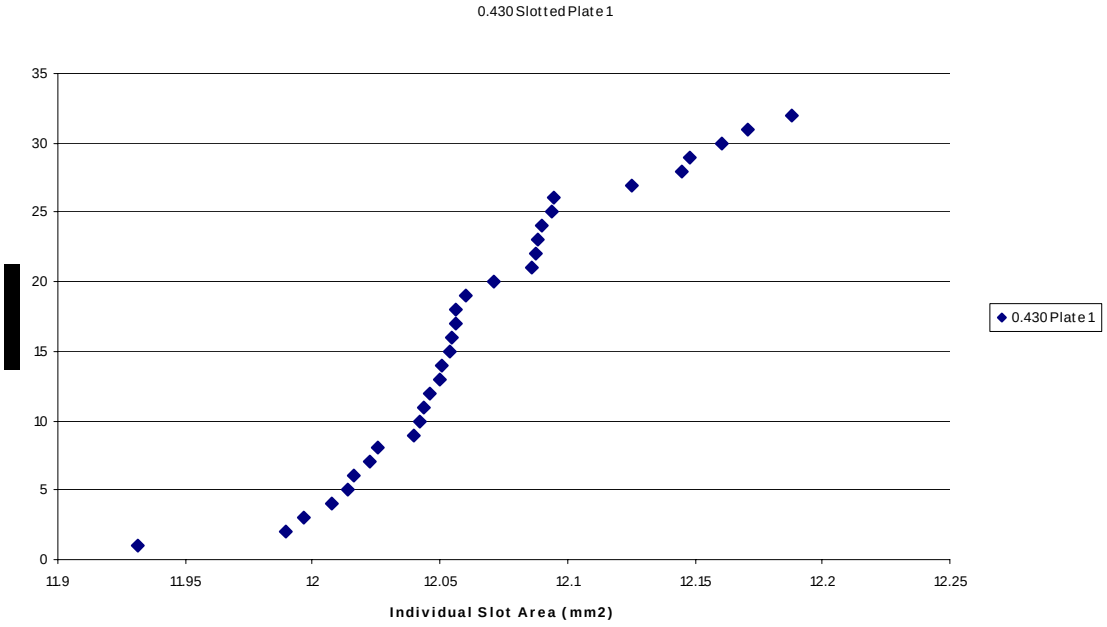

Figure 47: 0.430 Individual Slot Area Plate 1

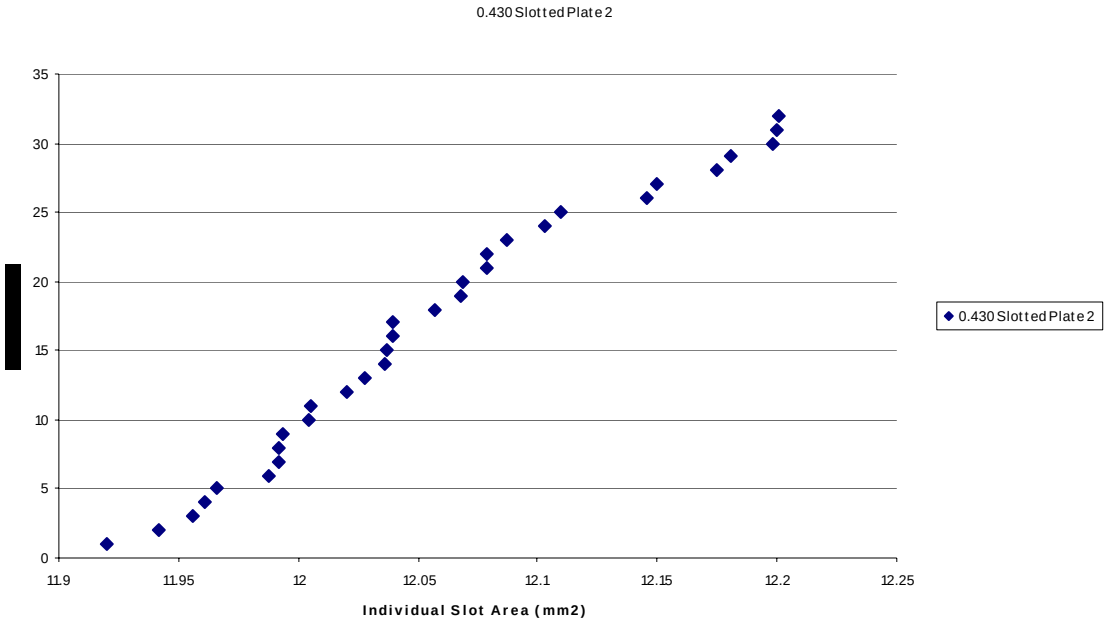

Figure 48: 0.430 Individual Slot Area Plate 2

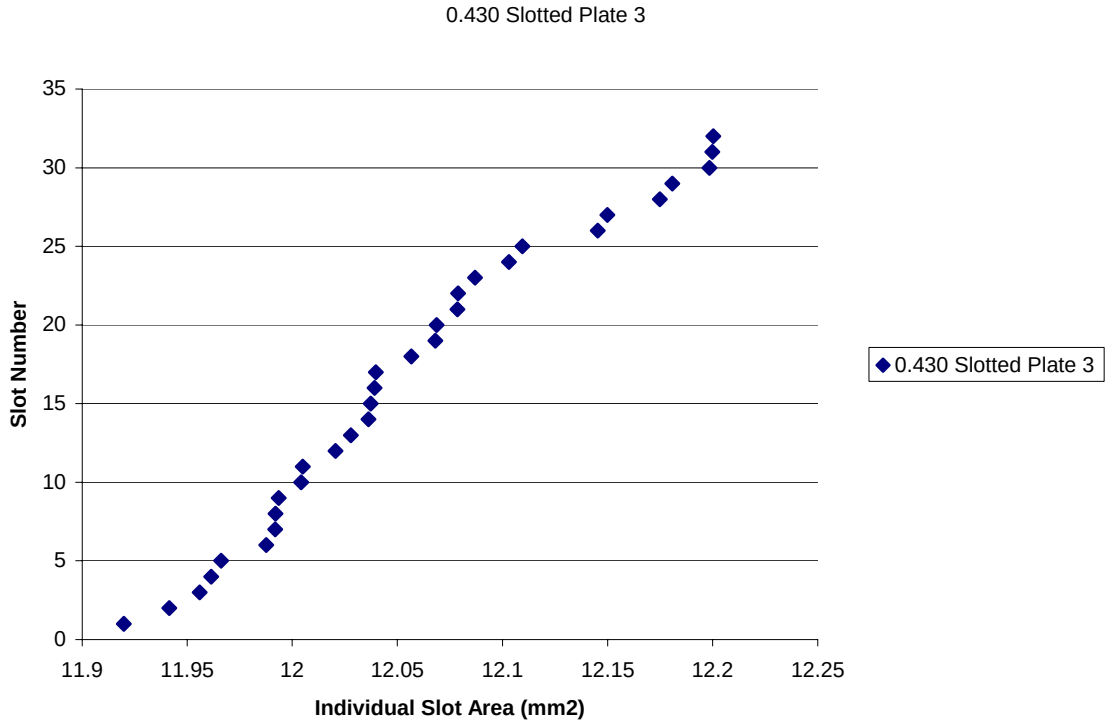

Figure 49: 0.430 Individual Slot Area Plate 3

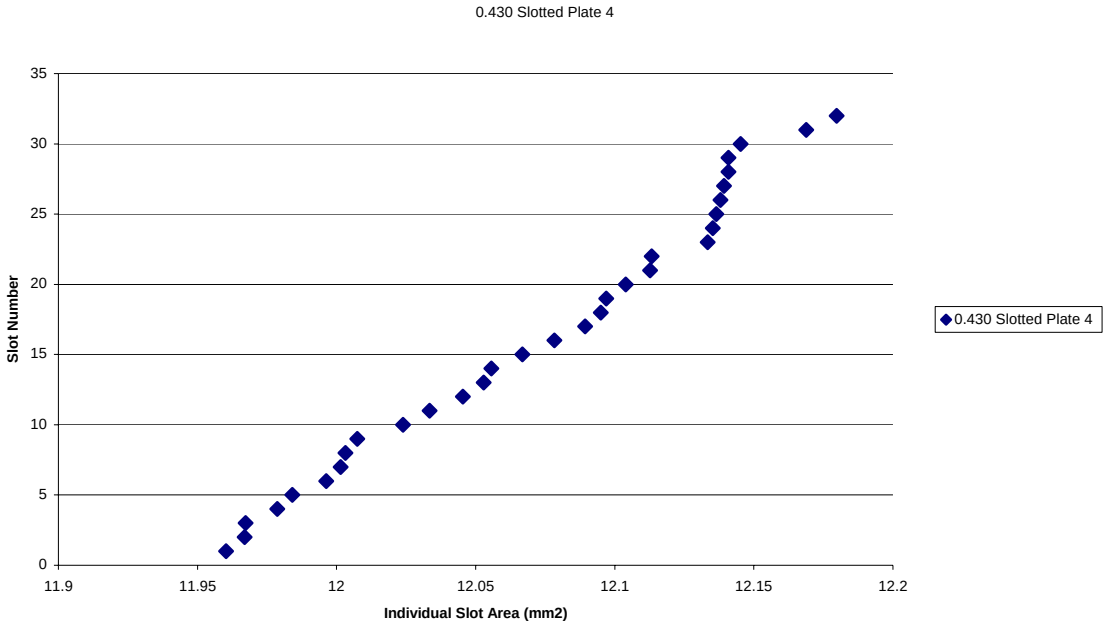

Figure 50: 0.430 Individual Slot Area Plate 4

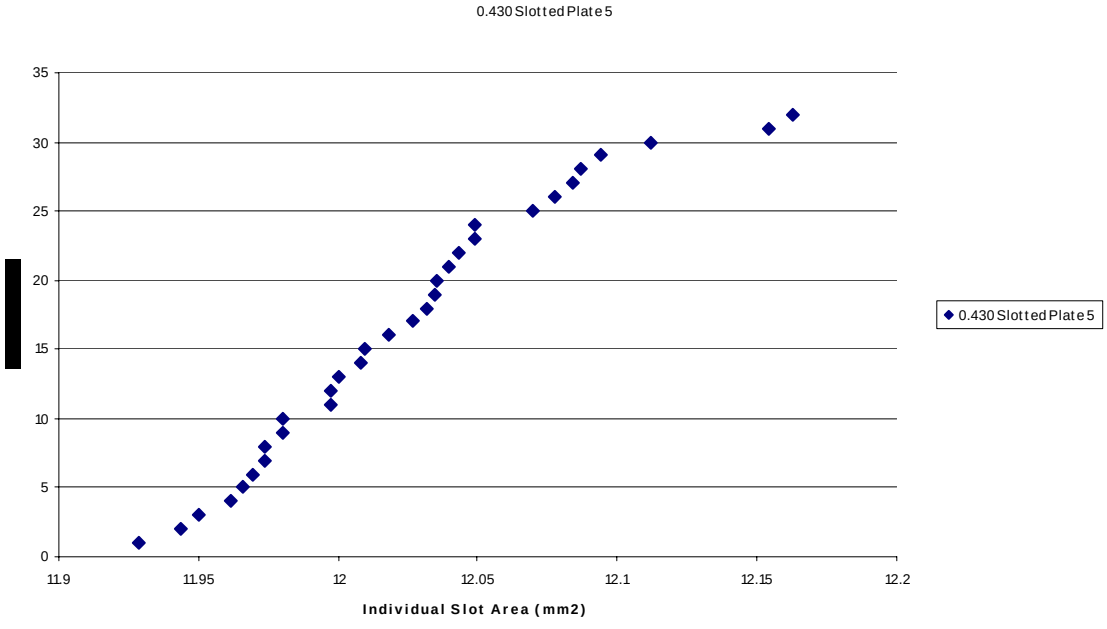

Figure 51: 0.430 Individual Slot Area Plate 5

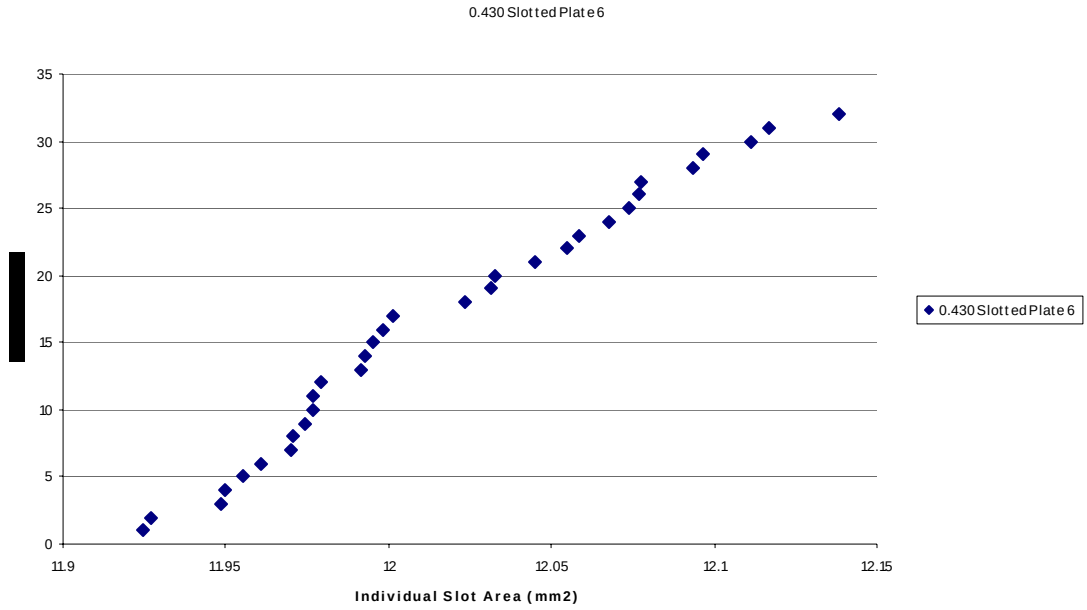

Figure 52: 0.430 Individual Slot Area Plate 6

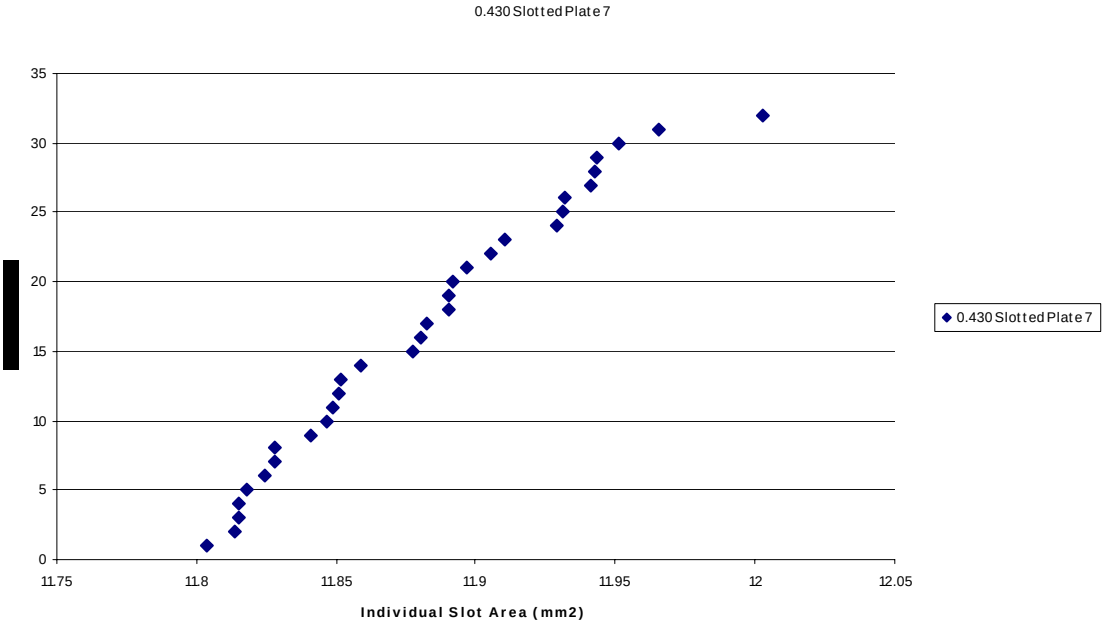

Figure 53: 0.430 Individual Slot Area Plate 7

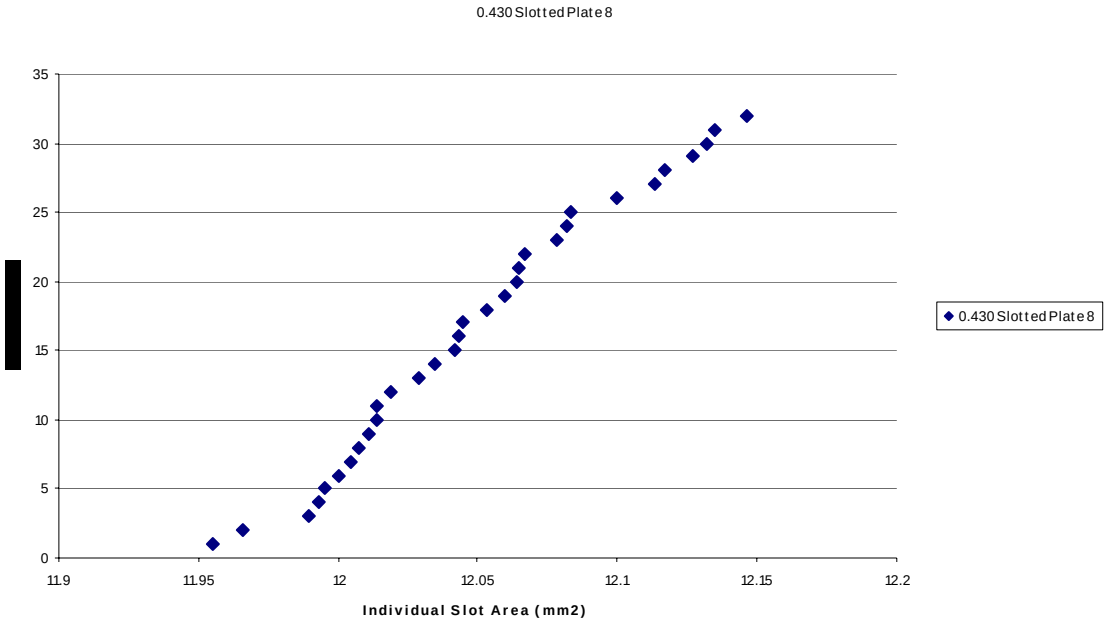

Figure 54: 0.430 Individual Slot Area Plate 8

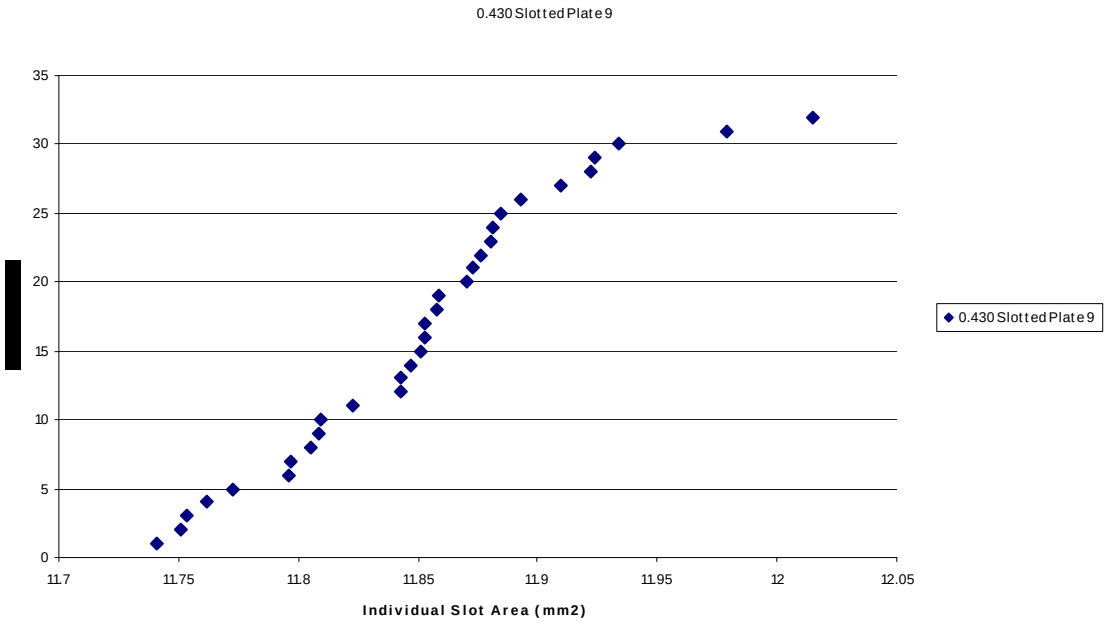

Figure 55: 0.430 Individual Slot Area Plate 9

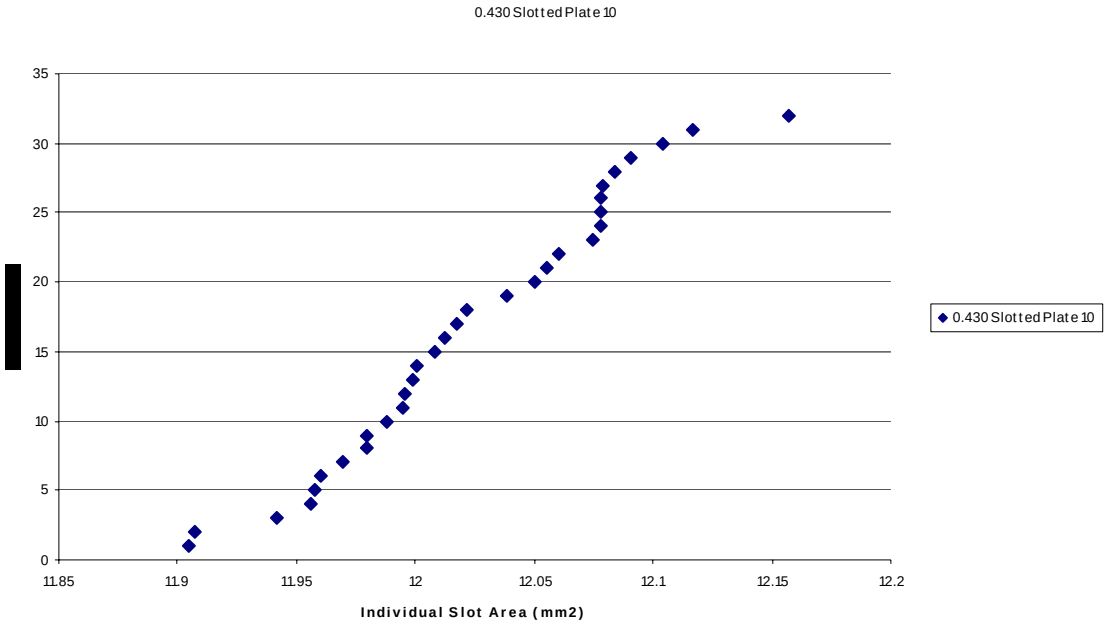

Figure 56: 0.430 Individual Slot Area Plate 10

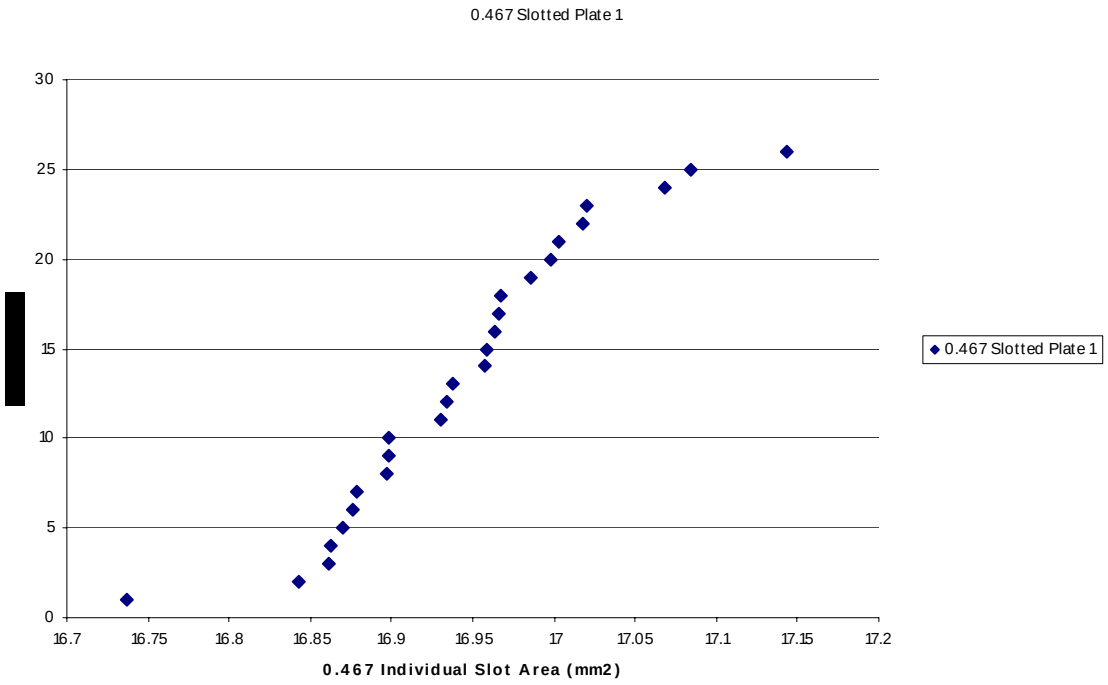

Figure 57: 0.467 Individual Slot Area Plate 1

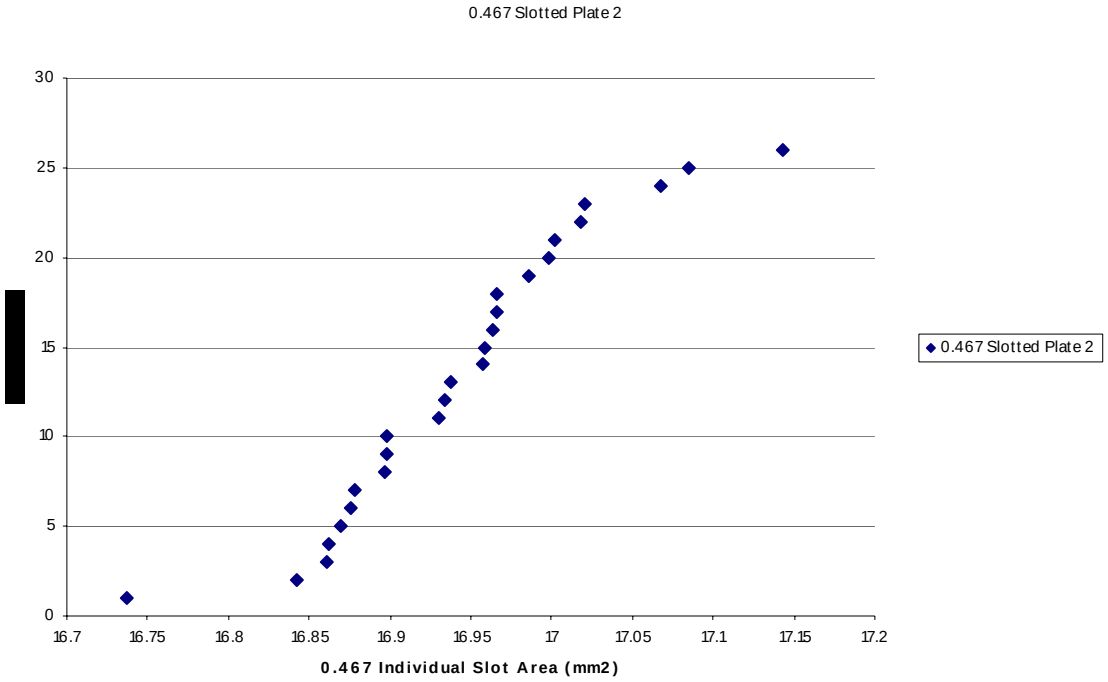

Figure 58: 0.467 Individual Slot Area Plate 2

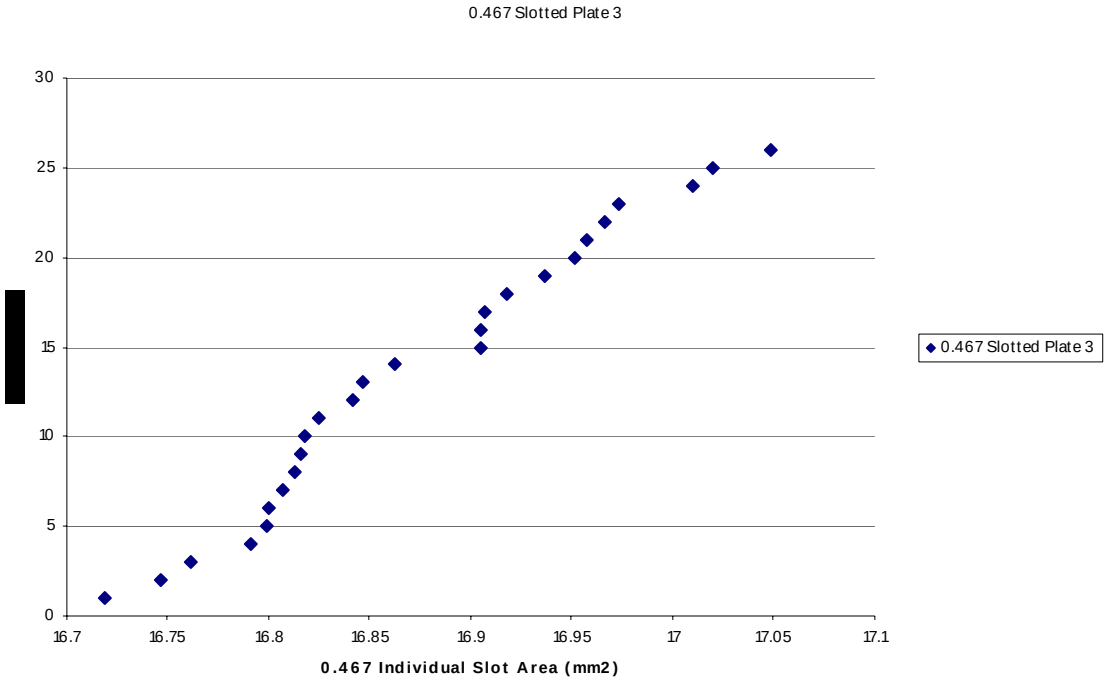

Figure 59: 0.467 Individual Area Plate 3

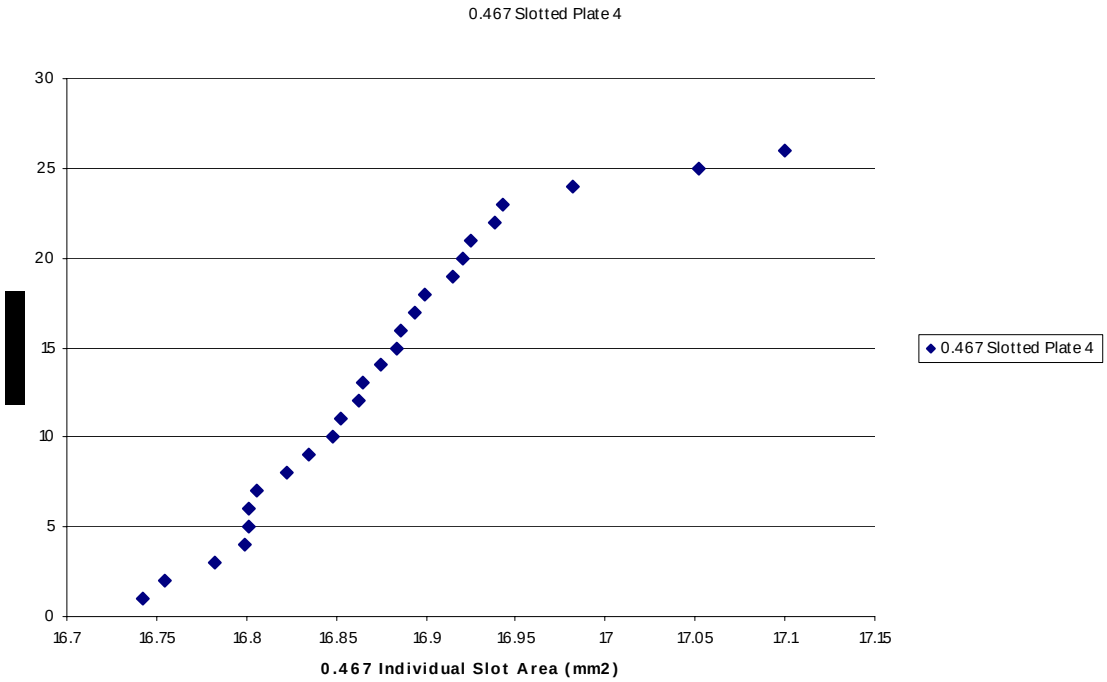

Figure 60: 0.467 Individual Slot Area Plate 4

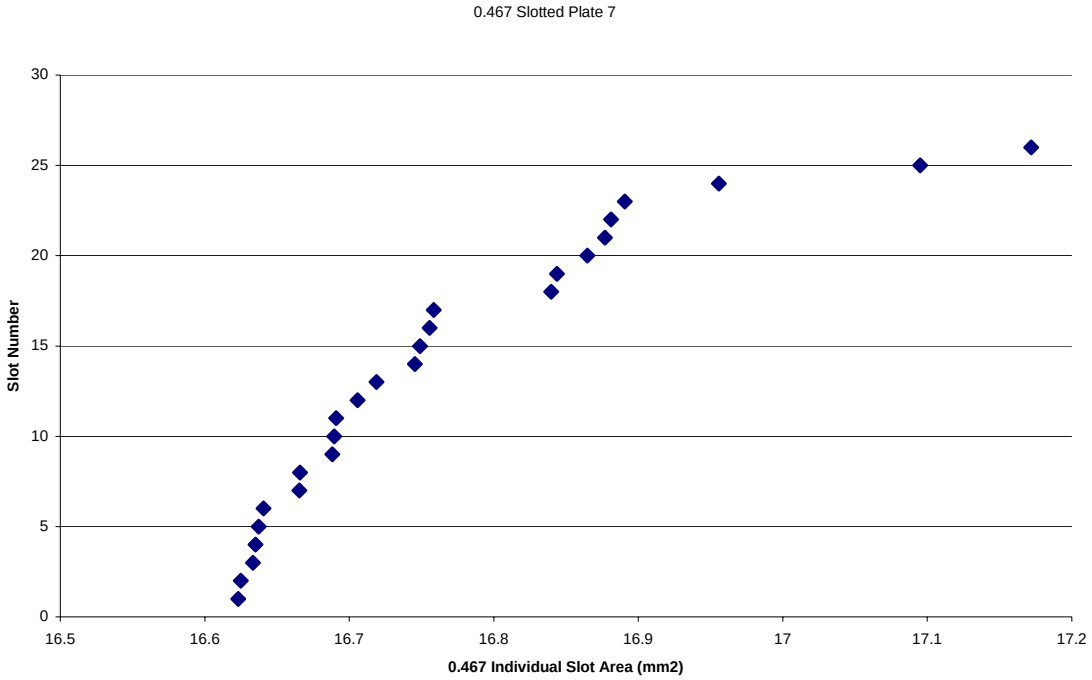

Figure 61: 0.467 Individual Slot Area Plate 7

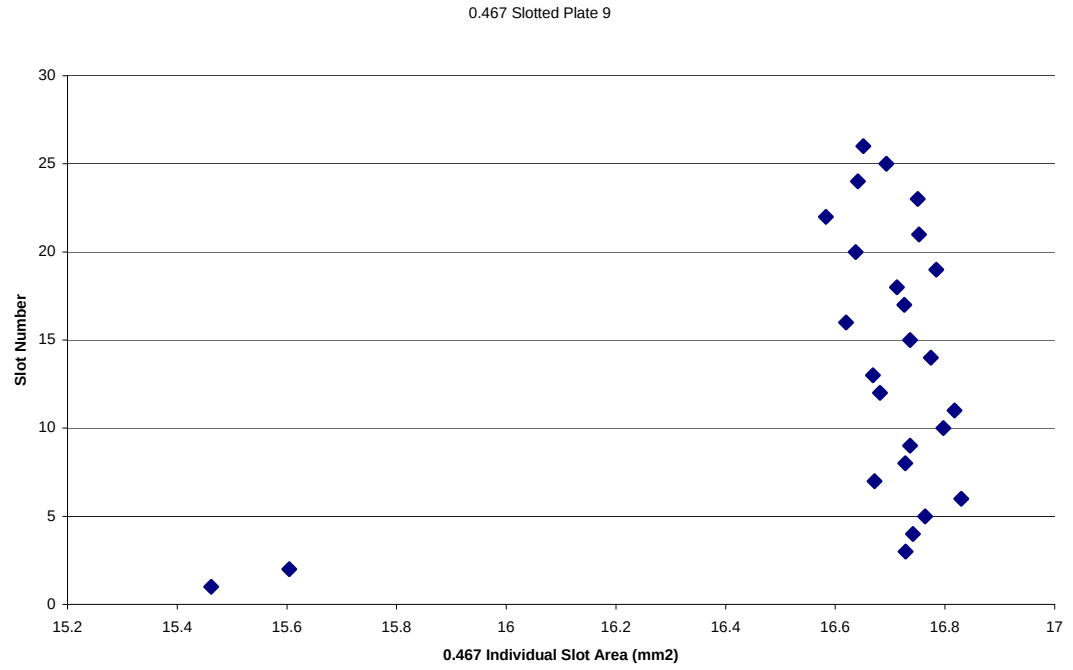

Figure 62: 0.467 Individual Slot Area Plate 9

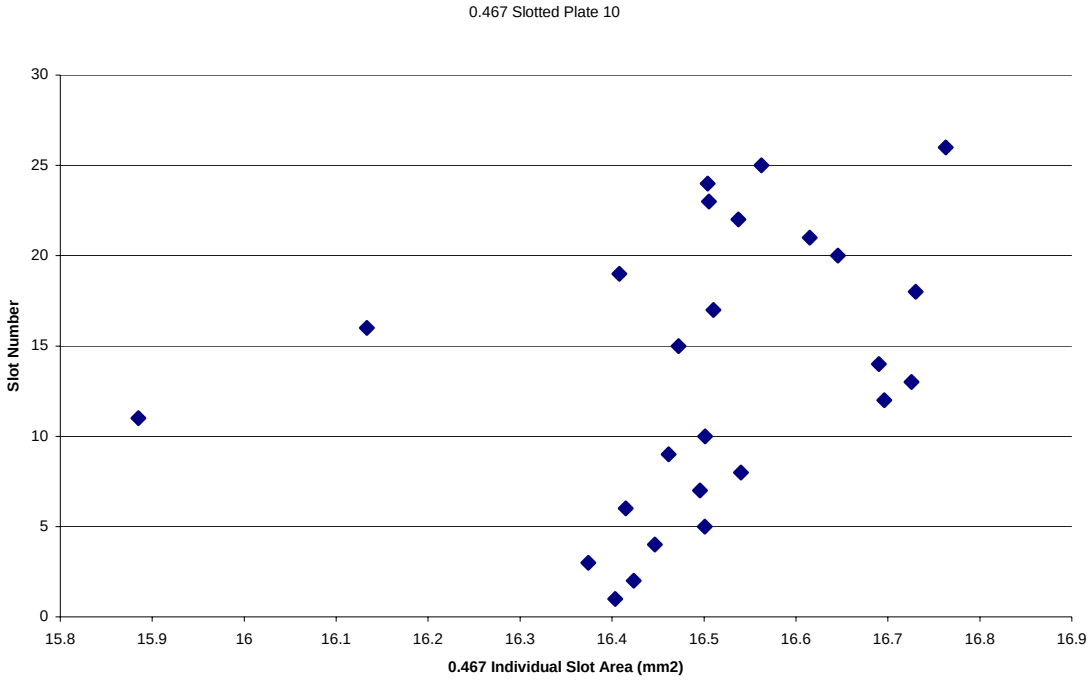

Figure 63: 0.467 Individual Slot Area Plate 10

APPENDIX B

TABLES

Table 1: 0.430 Beta Four Coefficient Data

Plate	1	2	3	4	6	7	8	9
a	0.963086	0.877722	0.911204	0.824656	0.808282	0.824566	0.777741	1.029431
b	0.387425	0.319112	0.418816	0.434485	0.450405	0.429219	0.358401	0.532396
c	0.489395	0.457604	0.626093	0.69467	0.718638	0.657419	0.544857	0.782402
d	2.317095	1.34478	2.076078	0.846376	0.784264	1.051675	0.48481	2.002242

Table 2: 0.467 Four Coefficient Data

Plate	2	4	7	9
a	1.002219	1.075848	0.96884	0.911206
b	0.834235	0.625756	0.733894	0.923375
c	1.10287	0.821774	0.933932	1.101954
d	1.080175	1.488781	0.734669	-0.04653

Table 3: 0.430 Three Coefficient Data

Plate	1	2	3	4	6	7	8
a	0.812108	0.754711	0.832737	0.765367	0.754044	0.751274	0.675326
b	0.869776	0.784956	0.828482	0.782616	0.76941	0.905484	0.761951
d	0.926715	0.024174	1.337698	0.12986	0.115173	0.170711	-0.92912

Table 4: 0.467 Three Coefficient Data

Plate	2	4	7	9
a	1.019997	0.994099	0.931972	0.931067
b	0.758802	0.84718	0.845921	0.838952
d	1.252613	0.719411	0.331016	0.189675

Table 5: Beta 0.430 C_d vs $\Delta P/P$ Coefficients

Plate:	8	3	6	4	1	2	7
a	0.728043	0.739416	0.746767	0.757031	0.749361	0.753182	0.740507
b	0.822599	0.721581	0.76103	0.772573	0.8134	0.783186	0.793114
R^2	0.955706	0.910858	0.975001	0.966015	0.907089	0.90166	0.966982

Table 6: Beta 0.467 C_d vs $\Delta P/P$ Coefficients

Plate:	2	4	7	9	7
a	0.915024	0.935387	0.906639	0.916537	0.905591
b	0.712221	0.818868	0.834675	0.831374	0.89124
R^2	0.933368	0.96758	0.926324	0.981765	0.858847

Table 7: Beta 0.467 Reynolds Number Coefficients

Plate:	2	4	7	9	7
a	1.057008	0.976412	0.913659	0.917112	0.889668
b	1.611667	0.524427	0.107032	0.017419	-0.18195
R^2	0.940363	0.970563	0.925972	0.981475	0.852978

Table 8: Beta 0.43 Reynolds Number Coefficients

Plate:	8	3	6	1	2
a	0.68325	0.812903	0.758935	0.772548	0.753179
b	-0.78613	1.091425	0.188211	0.390956	0.001095
R^2	0.961937	0.934391	0.975016	0.907571	0.901653

Table 9: Beta 0.430 Area Analysis

Plate	Intercepts	Area
8	0.724	0.59766
3	0.745	0.596859
7	0.745	0.590641
6	0.748	0.596116
2	0.750	0.598022
1	0.755	0.598461
4	0.762	0.598753

Table 10: Beta 0.467 Area Analysis

Plate	Intercept	Area
9	0.870	0.673135
7	0.910	0.675873
2	0.930	0.682859
4	0.935	0.680123

Table 11: 0.467 Individual Slot Area for Each Plate (mm^2)

	0.467 Plate Number (Area mm^2)							
	1	**2**	**3**	**4**	**5**	**7**	**9**	**10**
1	16.87765	16.73697	16.71905	16.74257	16.6794	16.62306	15.46222	16.40331
2	16.91764	16.84237	16.74649	16.75445	16.73731	16.62485	15.60458	16.42358
3	16.91999	16.86119	16.76128	16.78245	16.75769	16.63337	16.72813	16.37407
4	16.93836	16.8622	16.79063	16.79947	16.76531	16.63505	16.74168	16.44665
5	16.9434	16.86948	16.79947	16.80082	16.768	16.63729	16.76341	16.50086
6	16.94676	16.87553	16.80048	16.8016	16.78054	16.64065	16.8296	16.41495
7	16.95852	16.87877	16.80664	16.80619	16.7848	16.6654	16.67123	16.49571
8	16.99717	16.89647	16.81269	16.82255	16.79623	16.66585	16.72757	16.54018
9	16.99829	16.89782	16.8156	16.83509	16.79634	16.68825	16.73608	16.46144
10	17.00277	16.89793	16.81762	16.84764	16.80115	16.68959	16.7969	16.50131
11	17.01061	16.93007	16.82468	16.85301	16.80138	16.69083	16.81717	15.88505
12	17.01307	16.93422	16.84159	16.86242	16.81739	16.70584	16.68164	16.69609
13	17.01968	16.93747	16.84607	16.865	16.8221	16.71883	16.66843	16.72577
14	17.0199	16.95774	16.86265	16.87474	16.82815	16.74537	16.77394	16.69015
15	17.02024	16.95864	16.90498	16.88415	16.84752	16.74885	16.73619	16.47219
16	17.02976	16.96356	16.90532	16.88628	16.84764	16.75557	16.61959	16.13348
17	17.03122	16.96569	16.90689	16.89401	16.84842	16.75848	16.72589	16.51038
18	17.03872	16.9667	16.91831	16.8995	16.84909	16.83968	16.71256	16.73025
19	17.04858	16.98608	16.93702	16.9145	16.85122	16.84372	16.78402	16.40779
20	17.05373	16.9984	16.9518	16.92089	16.87161	16.86477	16.63706	16.64558
21	17.06482	17.00243	16.95707	16.92481	16.87183	16.87698	16.75243	16.61511
22	17.06583	17.01766	16.96659	16.9387	16.8958	16.88113	16.58285	16.53727
23	17.06885	17.02024	16.97353	16.94284	16.90431	16.89054	16.75019	16.50523
24	17.06997	17.06818	17.01005	16.98227	16.94139	16.95584	16.64132	16.504
25	17.07725	17.08431	17.02002	17.05205	16.95079	17.09495	16.69295	16.56258
26	17.09573	17.14333	17.04869	17.1001	16.9704	17.17178	16.65129	16.76274

Table 12: 0.430 Individual Slot Area for Each Plate (mm^2)

	0.430 Plate Number (Area mm^2)									
	1	**2**	**3**	**4**	**5**	**6**	**7**	**8**	**9**	**10**
1	11.9312	11.91978	11.85056	11.96033	11.92829	11.92471	11.8034	11.95495	11.74113	11.90499
2	11.98934	11.9414	11.91395	11.96693	11.94352	11.92706	11.81337	11.9657	11.7511	11.90701
3	11.99617	11.95585	11.9153	11.96727	11.95013	11.94868	11.81516	11.98967	11.75322	11.94184
4	12.00737	11.96133	11.94005	11.97869	11.96167	11.95002	11.8155	11.99292	11.76196	11.95596
5	12.01409	11.96615	11.94677	11.98407	11.96559	11.95506	11.8183	11.99527	11.77294	11.95775
6	12.01577	11.98766	11.96615	11.99628	11.9694	11.96077	11.82435	11.99998	11.79635	11.96021
7	12.02238	11.99191	11.96626	12.00143	11.97354	11.96996	11.82793	12.00479	11.79702	11.96917
8	12.0254	11.99202	11.97365	12.00322	11.97377	11.97074	11.82816	12.00759	11.80508	11.9797
9	12.03996	11.99359	11.97914	12.00748	11.97993	11.97433	11.84059	12.01106	11.80889	11.9797
10	12.04243	12.00423	12.00132	12.02383	11.98049	11.9769	11.84641	12.01364	11.80912	11.98799
11	12.04343	12.00502	12.00983	12.03347	11.99706	11.97701	11.84899	12.01409	11.82267	11.99449
12	12.04579	12.02047	12.01241	12.04545	11.99718	11.97914	11.85067	12.01879	11.84272	11.99527
13	12.04993	12.02787	12.01398	12.05284	12.00031	11.99124	11.85168	12.02899	11.84283	11.99897
14	12.05038	12.03627	12.01868	12.05564	12.00782	11.99247	11.85885	12.0347	11.84664	12.00098
15	12.05396	12.03727	12.02663	12.06684	12.00972	11.99494	11.8771	12.04198	11.85101	12.00793
16	12.0543	12.03918	12.02955	12.07827	12.01846	11.9983	11.88058	12.04343	11.85246	12.01252
17	12.05609	12.03974	12.0366	12.08936	12.02652	12.00121	11.88259	12.04478	11.85269	12.01767
18	12.05643	12.05665	12.05027	12.09496	12.03167	12.02327	11.89055	12.0534	11.8575	12.02193
19	12.0599	12.06808	12.05273	12.09697	12.03425	12.03156	11.89055	12.06001	11.85907	12.03839
20	12.07088	12.06864	12.05419	12.10392	12.03548	12.03268	11.89189	12.06416	11.87038	12.0506
21	12.08622	12.0786	12.05744	12.11265	12.03929	12.04523	11.89693	12.06494	11.8733	12.0552
22	12.08768	12.07894	12.06382	12.11322	12.04332	12.05475	11.90511	12.06662	11.87643	12.06001
23	12.08857	12.08701	12.08017	12.13338	12.0487	12.05833	11.91003	12.0786	11.88013	12.07457
24	12.09014	12.10313	12.08521	12.13528	12.04904	12.06785	11.92874	12.08219	11.88158	12.0776
25	12.09395	12.10952	12.09261	12.13651	12.06953	12.07401	11.93132	12.08353	11.88461	12.07804
26	12.0944	12.14536	12.09653	12.13797	12.0776	12.0767	11.93221	12.1	11.89335	12.07804
27	12.1252	12.14995	12.10123	12.13931	12.08387	12.07726	11.94106	12.1131	11.90981	12.07916
28	12.1448	12.17482	12.10403	12.14088	12.08701	12.09361	11.94285	12.11691	11.92247	12.08353
29	12.14783	12.18076	12.1271	12.14088	12.09406	12.09653	11.94352	12.12699	11.92381	12.0907
30	12.16037	12.19856	12.13685	12.14525	12.11198	12.1112	11.95092	12.13226	11.934	12.10414
31	12.17056	12.1998	12.14032	12.16888	12.15432	12.11669	11.96537	12.13494	11.97903	12.1168
32	12.18792	12.20036	12.22589	12.17975	12.16306	12.1383	12.00255	12.14637	12.0151	12.15679

APPENDIX C

VIDEO

The air/oil visualization video for the slotted orifice plate and standard orifice plate comparison are included. The air/water visualization video for the slotted orifice plate, standard orifice and V-Cone comparisons are also included with this document as mpg files that can be viewed with computer video software.

VITA

Sara A. Sparks is the daughter of Gregory E. and Theresa J. Sparks. She was born on January 9, 1979 in Waterloo, Iowa. She has a brother, James. She graduated from Hudson High School in 1997. In 2002, she received her Bachelor of Science degree in mechanical engineering from Iowa State University in Ames, Iowa. She enrolled in the Master of Science program in mechanical engineering at Texas A&M University in 2002. Her permanent mailing address is: 451 Primrose Drive, Hudson, Iowa, 50643.